



Search for supersymmetry in events with one lepton and multiple jets in proton-proton collisions at $\sqrt{s} = 13$ TeV

The CMS Collaboration*

Abstract

A search for supersymmetry is performed in events with a single electron or muon in proton-proton collisions at a center-of-mass energy of 13 TeV. The data were recorded by the CMS experiment at the LHC and correspond to an integrated luminosity of 2.3 fb^{-1} . Several exclusive search regions are defined based on the number of jets and b-tagged jets, the scalar sum of the jet transverse momenta, and the scalar sum of the missing transverse momentum and the transverse momentum of the lepton. The observed event yields in data are consistent with the expected backgrounds from standard model processes. The results are interpreted using two simplified models of supersymmetric particle spectra, both of which describe gluino pair production. In the first model, each gluino decays via a three-body process to top quarks and a neutralino, which is associated with the observed missing transverse momentum in the event. Gluinos with masses up to 1.6 TeV are excluded for neutralino masses below 600 GeV. In the second model, each gluino decays via a three-body process to two light quarks and a chargino, which subsequently decays to a W boson and a neutralino. The mass of the chargino is taken to be midway between the gluino and neutralino masses. In this model, gluinos with masses below 1.4 TeV are excluded for neutralino masses below 700 GeV.

Published in Physical Review D as doi:10.1103/PhysRevD.95.012011.

1 Introduction

Supersymmetry (SUSY) [1–8] is a well-motivated theoretical framework that postulates new physics beyond the standard model (SM). Models based on SUSY can address several open questions in particle physics, e.g. the cancellation of quadratically divergent loop corrections when calculating the squared mass of the Higgs boson. In R -parity [9] conserving SUSY models, the lightest SUSY particle (LSP) is stable and can be a viable dark matter candidate. An inclusive search for SUSY in the single-lepton channel was performed with 13 TeV data recorded in 2015 by the CMS experiment at the CERN LHC, corresponding to an integrated luminosity of 2.3 fb^{-1} . Similar searches were performed in 7 TeV [10–12] and in 8 TeV [13–15] data by the CMS and ATLAS experiments. First results in the single-lepton final state at 13 TeV are also available from both collaborations [16–18]. In this paper, we present a search for gluino pair production designed to be sensitive to a variety of SUSY models.

In this analysis, the main backgrounds arise from W +jets events and top quark-antiquark ($t\bar{t}$ +jets) events, which also lead to W -boson production. In W +jets events, or in $t\bar{t}$ +jets events with a single leptonic W -boson decay, the missing transverse momentum, \vec{p}_T^{miss} , defined as the negative vector sum of the transverse momenta of all reconstructed particles in the event, provides a measurement of the neutrino transverse momentum. The quantity $\vec{p}_T^\ell + \vec{p}_T^{\text{miss}}$, where \vec{p}_T^ℓ is the lepton transverse momentum vector, corresponds to the transverse momentum of the W boson in background events of this type. We also define the magnitude of the missing transverse momentum, $E_T^{\text{miss}} = |\vec{p}_T^{\text{miss}}|$, and the sum $L_T = p_T^\ell + E_T^{\text{miss}}$, where p_T^ℓ is the magnitude of \vec{p}_T^ℓ .

A key analysis variable is the azimuthal angle $\Delta\Phi$, measured in the plane perpendicular to the beams, between \vec{p}_T^ℓ and $\vec{p}_T^\ell + \vec{p}_T^{\text{miss}}$. In background events with a single W -boson decay, $\Delta\Phi$ corresponds to the azimuthal angle between the transverse momentum vectors of the charged lepton and the W boson. In such events, the distribution of $\Delta\Phi$ falls rapidly and has a maximum value determined by the mass and transverse momentum of the W boson. The higher the boost of the W boson, the smaller the maximum value of $\Delta\Phi$. In SUSY events corresponding to our signal models, however, E_T^{miss} typically receives a large contribution from the missing momentum of the two neutralino LSPs. As a consequence, the $\Delta\Phi$ distribution in signal events is roughly uniform. The main backgrounds can therefore be suppressed by rejecting events with a small value of $\Delta\Phi$. The primary remaining background arises from $t\bar{t}$ +jets production where both W bosons decay into a charged lepton and a neutrino, with one lepton being not well identified or falling outside the detector acceptance. This background populates the high region of $\Delta\Phi$.

Since many models of gluino pair production lead to final states with a large number of jets, the signal-to-background ratio is very small in regions with low jet multiplicity. We therefore restrict the search to regions of large jet multiplicity and use low jet multiplicity regions, dominantly populated by events from SM processes, to estimate the background. Exclusive search regions are characterized by the number of jets (n_{jet}), the number of b -tagged jets (n_b), the scalar sum of the transverse momenta p_T of the jets (H_T), and L_T .

The results are interpreted in terms of simplified models [19–22] of gluino pair production. In the first model, designated T1tttt and shown in Fig. 1 (left), gluinos are pair produced and subsequently undergo three-body decays to $t\bar{t} + \tilde{\chi}_1^0$, where $\tilde{\chi}_1^0$ is the lightest neutralino. In the second model, termed T5qqqWW and shown in Fig. 1 (right), the gluinos undergo three-body decays to a quark-antiquark pair ($q\bar{q}$) from the first or second generation and a chargino ($\tilde{\chi}_1^\pm$). The chargino mass is taken to be $m_{\tilde{\chi}_1^\pm} = 0.5(m_{\tilde{g}} + m_{\tilde{\chi}_1^0})$. The chargino then decays to a W boson

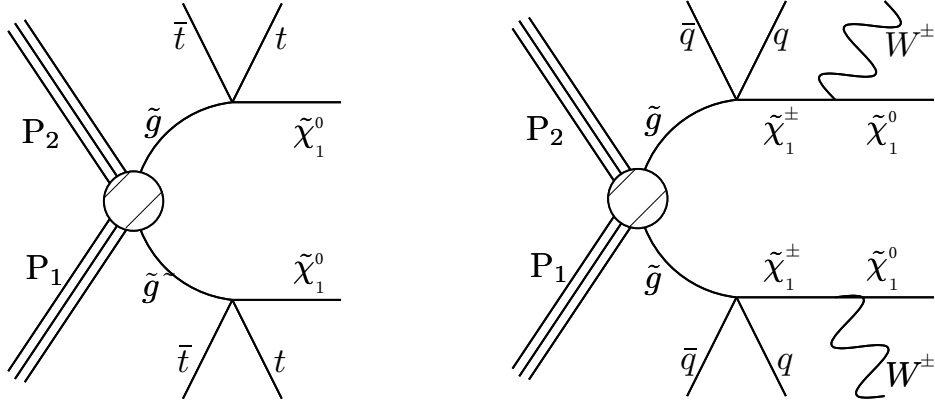


Figure 1: Diagrams showing the simplified models (left) T1tttt and (right) T5qqqqWW. Depending on the mass difference between the chargino ($\tilde{\chi}_1^\pm$) and the neutralino ($\tilde{\chi}_1^0$), the W boson can be virtual.

and the $\tilde{\chi}_1^0$, where the W boson can be virtual, depending on the mass difference between the chargino and the lightest neutralino.

The organization of this paper is as follows. Section 2 describes the CMS detector. The event reconstruction and selection are discussed in Sections 3 and 4, respectively. The background estimations are given in Section 5. An overview of the main systematic uncertainties is presented in Section 6. The results are discussed and interpreted in Section 7, and a summary is given in Section 8.

2 The CMS detector

The central feature of the CMS apparatus is a superconducting solenoid of 6 m internal diameter, providing a magnetic field of 3.8 T. A silicon pixel and strip tracker, a lead tungstate crystal electromagnetic calorimeter (ECAL), and a brass and scintillator hadron calorimeter (HCAL), each composed of a barrel and two endcap sections, reside within the solenoid volume. Forward calorimeters extend the pseudorapidity (η) [23] coverage provided by the barrel and endcap detectors. Muons are measured in the range $|\eta| < 2.4$, with detection planes made using three technologies: drift tubes, cathode strip chambers, and resistive plate chambers.

The silicon tracker measures charged particles within the range $|\eta| < 2.5$. Isolated particles with transverse momenta $p_T = 100$ GeV, emitted at $|\eta| < 1.4$, have track resolutions of 2.8% in p_T , and 10 (30) μm in the transverse (longitudinal) impact parameter [24]. The ECAL and HCAL measure energy depositions in the range $|\eta| < 3$, with quartz fibre and steel forward calorimeters extending the coverage to $|\eta| < 5$. When information from the various detector systems is combined, the resulting jet energy resolution is typically 15% at 10 GeV, 8% at 100 GeV, and 4% at 1 TeV [25]. The momentum resolution for electrons with $p_T \approx 45$ GeV from $Z \rightarrow ee$ decays ranges from 1.7% for electrons that do not shower in the barrel region, to 4.5% for electrons that shower in the endcaps [26]. Matching muons to tracks measured in the silicon tracker yields relative transverse momentum resolutions for muons with $20 < p_T < 100$ GeV of 1.3–2.0% in the barrel, and less than 6% in the endcaps. The p_T resolution in the barrel is below 10% for muons with p_T up to 1 TeV [27].

The CMS trigger system consists of two levels, where the first level (L1), composed of custom hardware processors, uses information from the calorimeters and muon detectors to select the most interesting events in a fixed time interval of less than 4 μs . The high-level trigger (HLT)

processor farm further decreases the event rate from around 100 kHz to less than 1 kHz, before data storage.

A more detailed description of the CMS detector, together with a definition of the coordinate system used and the relevant kinematic variables, can be found in Ref. [23].

3 Event reconstruction and simulation

All objects in the event are reconstructed using the particle-flow event reconstruction algorithm [28, 29], which reconstructs and identifies each individual particle through an optimized combination of information from the various elements of the CMS detector. The energy of electrons is determined from a combination of the electron momentum at the primary interaction vertex as determined by the tracker, the energy of the corresponding ECAL cluster, and the energy sum of all bremsstrahlung photons spatially compatible with originating from the electron track [26]. Electron candidates are required to satisfy identification criteria designed to suppress contributions from misidentified jets, photon conversions, and electrons from heavy-flavor quark decays. Muons are reconstructed using a stand-alone muon track in the muon system serving as a seed to find a corresponding track in the silicon detector [27]. Additional criteria include requirements on the track and hit parameters. Events are vetoed if additional electrons or muons with looser identification requirements are found.

The degree of isolation of a lepton from other particles provides a strong indication of whether it was produced in a hadronic jet, such as a jet resulting from the fragmentation of a b quark, or in the leptonic decay of a W boson or other heavy particle. Lepton isolation is quantified by performing a scalar sum of the transverse momenta of all particles that lie within a cone of specified size around the lepton momentum vector, excluding the contribution of the lepton itself. To maintain high efficiency for signal events, which typically contain a large number of jets from the SUSY decay chains, we use a p_T -dependent cone radius $R = (0.2, 10 \text{ GeV}/p_T[\text{GeV}], 0.05)$ for $(p_T < 50 \text{ GeV}, 50 \text{ GeV} < p_T < 200 \text{ GeV}, p_T > 200 \text{ GeV})$, respectively. The isolation variable is defined as a relative quantity, I_{rel} , by dividing this scalar sum by the p_T of the lepton. For selected muons or electrons, we require $I_{\text{rel}} < 0.2$ and $I_{\text{rel}} < 0.1$, respectively, while for additional leptons used in the event veto, we require $I_{\text{rel}} < 0.4$. When computing the isolation variable, an area-based correction is applied to remove the contribution of particles from additional proton-proton collisions within the same or neighboring bunch crossings (pileup).

The energy of charged hadrons is determined from a combination of their momenta measured in the tracker and the matching ECAL and HCAL energy depositions, corrected for zero-suppression effects in the readout electronics, and for the response function of the calorimeters to hadronic showers. Finally, the energy of neutral hadrons is obtained from the corresponding corrected ECAL and HCAL energies.

Jets are clustered with the anti- k_T algorithm [30] with a distance parameter of 0.4 [25], as implemented in the FASTJET package [31]. Jet momentum is determined as the vectorial sum of all particle momenta in the jet. An offset is subtracted from the jet energies to take into account the contribution from pileup [32]. Jet energy corrections are obtained from simulation, and are confirmed with in situ measurements of the energy balance in dijet and photon+jet events [25]. Additional selection criteria are applied to each event to remove spurious jet-like features originating from isolated noise patterns in certain HCAL regions.

To identify jets originating from b quarks, we use an inclusive combined secondary vertex tagger (CSVv2) [33, 34], which employs both secondary vertex and track-based information.

The working point is chosen to have about 70% b tagging efficiency and a 1.5% light-flavor misidentification rate [35]. Double counting of objects is avoided by not considering jets that lie within a cone of radius 0.4 around a selected lepton.

While the main backgrounds are determined from data, as described in Section 5, simulated events are used to validate the techniques, and to estimate extrapolation factors as needed. In addition, some smaller backgrounds are estimated entirely from simulation. The leading-order (LO) MADGRAPH5 [36] event generator, using the NNPDF3.0LO [37] parton distribution functions (PDFs), is used to simulate $t\bar{t}$ +jets, W +jets, Z +jets, and multijet events. Single-top quark events in the t -channel and the tW process are generated using the next-to-leading order (NLO) POWHEGv1.0 [38–42] program, and in the s -channel process, as well as for $t\bar{t}W$ and $t\bar{t}Z$ production, using NLO MADGRAPH5_aMC@NLO [43]. All signal events are generated with MADGRAPH5, with up to two partons in addition to the gluino pair. Both programs use the NNPDF3.0NLO [37] PDF. The gluino decays are based on a pure phase-space matrix element [44], with signal production cross sections [45–49] computed at NLO plus next-to-leading-logarithm (NLL) accuracy.

We define several benchmark points: the model T1tttt(1.2,0.8) (T1tttt(1.5,0.1)) corresponds to a gluino mass of 1.2 (1.5) TeV and neutralino mass of 0.8 (0.1) TeV, respectively. The model T5qqqqWW(1.0,0.7) (T5qqqqWW(1.2,0.8) and T5qqqqWW(1.5,0.1)) corresponds to a gluino mass of 1.0 (1.2 and 1.5) TeV and neutralino mass of 0.7 (0.8 and 0.1) TeV. For the latter, the intermediate chargino mass is fixed at 0.85 (1.0 and 0.8) TeV.

Showering and hadronization of all partons is performed using the PYTHIA 8.2 package [44]. Pileup is generated for some nominal distribution of the number of proton-proton interactions per bunch crossing, which is weighted to match the corresponding distribution in data. The detector response for all backgrounds is modelled using the GEANT4 [50] package, while for the signal the CMS fast simulation program [51] is used to reduce computation time. The fast simulation has been validated against the detailed GEANT4-based simulation for the variables relevant for this search, and efficiency corrections based on measurements in data are applied.

4 Trigger and event selection

The events are selected with an L1 trigger requiring $H_T > 150$ GeV, followed by HLT requirements of $H_T > 350$ GeV (online reconstruction) and at least one isolated lepton (an electron or muon) satisfying $p_T > 15$ GeV. A trigger efficiency of $94 \pm 1\%$ is observed in the kinematic regime of the analysis, defined by lepton $p_T > 25$ GeV and $H_T > 500$ GeV, where the trigger efficiency reaches its maximum.

The electron or muon candidate is required to have a minimum p_T of 25 GeV. Events with additional electrons or muons with $p_T > 10$ GeV, satisfying the criteria for vetoed leptons, are rejected. Jets are selected with $p_T > 30$ GeV and $|\eta| < 2.4$. In all search regions we require at least five jets, where the two highest- p_T jets must satisfy $p_T > 80$ GeV.

To separate possible new-physics signals from background, we use the L_T variable, which is defined as the scalar sum of the lepton p_T and the missing transverse energy E_T^{miss} , and reflects the leptonic energy scale of the event. A minimum L_T of 250 GeV is required, such that the analysis is not only sensitive to events with high E_T^{miss} , but also to signal events with very small E_T^{miss} , but higher lepton p_T . An additional kinematic quantity important for the search is given by the hadronic energy scale of the event H_T . A cutflow for the benchmark signal models is given in Table 1.

Table 1: Expected event yields for SUSY signal benchmark models, normalized to 2.3 fb^{-1} . The baseline selection corresponds to all requirements up to and including the requirement on L_T . The last two lines are exclusive for the zero-b and the multi-b selection, respectively. The events are corrected with scale factors to account for differences in the lepton identification and isolation efficiencies, trigger efficiency, and the b-tagging efficiency between simulation and data.

Selection	T1tttt (1.2,0.8)	T1tttt (1.5,0.1)	T5qqqqWW (1.2,0.8)	T5qqqqWW (1.5,0.1)
All events	178	30	185	31
One hard lepton	55	11	51	9.3
No veto lepton	45	9.1	47	8.8
$n_{\text{jet}} \geq 5$	44	8.9	36	8.1
$p_T(\text{jet } 2) > 80 \text{ GeV}$	36	8.9	34	8.1
$H_T > 500 \text{ GeV}$	30	8.9	27	8.1
$L_T > 250 \text{ GeV}$	15	8.4	21	7.8
$n_b = 0$ and $\Delta\Phi > 0.75$	0.47	0.26	11	3.5
$n_b \geq 1$, $n_{\text{jet}} \geq 6$ and $\Delta\Phi > 0.75$	9.3	5.1	2.9	1.2

After imposing the minimum requirements on L_T and H_T , several search regions are defined in bins of n_{jet} , n_b , L_T , and H_T , where n_{jet} and n_b are the numbers of jets and b-tagged jets, respectively. Defining search bins in b-jet multiplicity enables the analysis to target specific event topologies and to separate them from SM backgrounds. The phase space is divided into exclusive $[0, 1, 2, \geq 3]$ b-tagged jet categories when defining search bins, with a minimum b-jet p_T of 30 GeV.

All search bins with at least one b-tagged jet, called in the following “multi-b” bins, are sensitive to the T1tttt model, while the search bins requiring zero b-tagged jets, called “zero-b” bins, are sensitive to the T5qqqqWW model. The baseline selection and the background estimation method differ for these two b-tag categories. For T1tttt, we expect a large number of jets and find in simulation that the n_{jet} distribution peaks at eight jets for most mass points. We require at least six jets for the multi-b analysis and define two independent categories with 6–8 and ≥ 9 jets. For the zero-b analysis, where the investigated simplified T5qqqqWW model has fewer jets, we require in the search region 5, 6–7, or ≥ 8 jets. Depending on the specific SUSY particle masses, the hadronic event activity varies. To accommodate this, we define search bins in H_T . Figure 2 shows the H_T distributions for the multi-b and the zero-b selection. To exploit the strong separation power associated with the L_T variable, we divide the search region into four bins in L_T , such that sufficient statistical accuracy is given in each control bin to predict the background in the corresponding search bin.

After these selections, the main backgrounds are leptonically decaying W+jets and semi-leptonic $t\bar{t}$ events. These backgrounds, both of which contain one lepton and one neutrino (from the W boson decay) in the final state, are mostly located at small $\Delta\Phi$ values due to the correlation between the lepton and the neutrino. Therefore, the region with large $\Delta\Phi$ is defined as the search region, while the events with small $\Delta\Phi$ are used as the control sample. Figure 3 shows the $\Delta\Phi$ distributions for the zero-b and multi-b search regions. The ratio of the background event yield in the search region to that in the control region is determined in the corresponding signal-depleted sideband regions, which have smaller values of n_{jet} , as discussed in Section 5. Since the angle between the W boson and the lepton depends on the W momentum, being smaller for W bosons with higher boost, the $\Delta\Phi$ requirement for the signal region is chosen depending on L_T , which is a measure of the W boson p_T . For the zero-b analysis, $\Delta\Phi$ is required to be larger

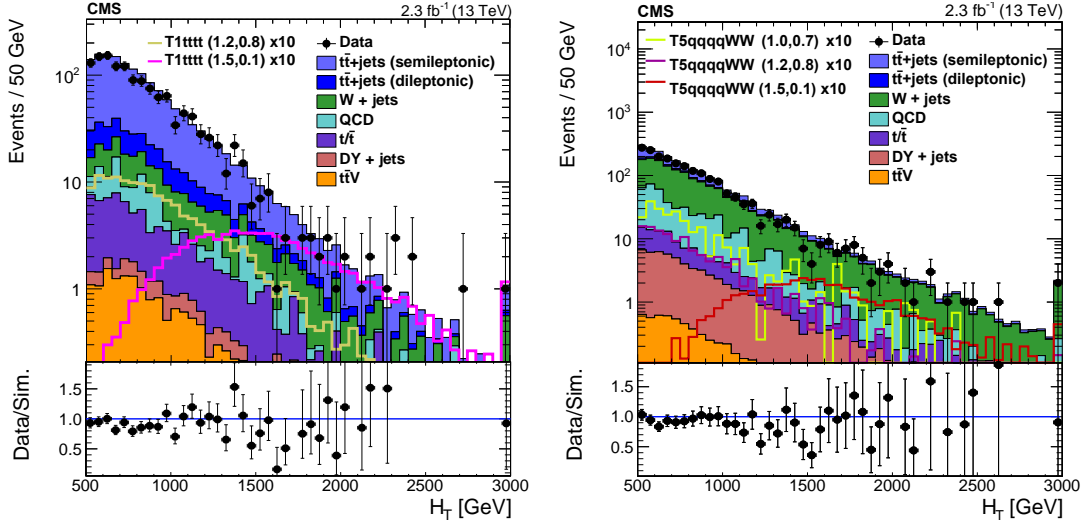


Figure 2: The H_T distribution for (left) the multi-b analysis and (right) the zero-b analysis, both after the baseline selection. The simulated background events are stacked on top of each other, and several signal points are overlaid for illustration, but without stacking. Overflows are included in the last bin. The label DY refers to $q\bar{q} \rightarrow Z/\gamma^* \rightarrow \ell^+\ell^-$ events, and QCD refers to multijet events. The event yields for the benchmark models have been scaled up by a factor of 10. The ratio of data to simulation is given below each of the panels. All uncertainties are statistical only.

than 1.0 for most regions except for those with large L_T , where the requirement is relaxed to 0.75, while the multi-b analysis has a relaxed $\Delta\Phi$ requirement of 0.75 and 0.5 for medium- and high- L_T regions, respectively.

In total, we define 30 search bins in the multi-b analysis and 13 search bins in the zero-b analysis, as described in detail in Table 2.

Table 2: Search regions and the corresponding minimum $\Delta\Phi$ requirements.

n_{jet}	n_b	L_T [GeV]	H_T [GeV]	$\Delta\Phi$ [rad]
[6,8]	=1, =2, ≥ 3	[250, 350]	[500, 750], ≥ 750	1.0
		[350, 450]	[500, 750], ≥ 750	0.75
	=1, ≥ 2	[450, 600]	[500, 1250], ≥ 1250	0.75
		≥ 600	[500, 1250], ≥ 1250	0.5
≥ 9	=1, =2	[250, 350]	[500, 1250], ≥ 1250	1.0
		≥ 3	≥ 500	1.0
	=1, =2, ≥ 3	[350, 450]	≥ 500	0.75
		=1, ≥ 2	≥ 450	≥ 500
5		[250, 350], [350, 450], ≥ 450	≥ 500	1.0
[6,7]	0	[250, 350], [350, 450]	[500, 750], ≥ 750	0.75
		≥ 450	[500, 1000], ≥ 1000	
≥ 8		[250, 350]	[500, 750], ≥ 750	1.0
		[350, 450], ≥ 450	≥ 500	0.75

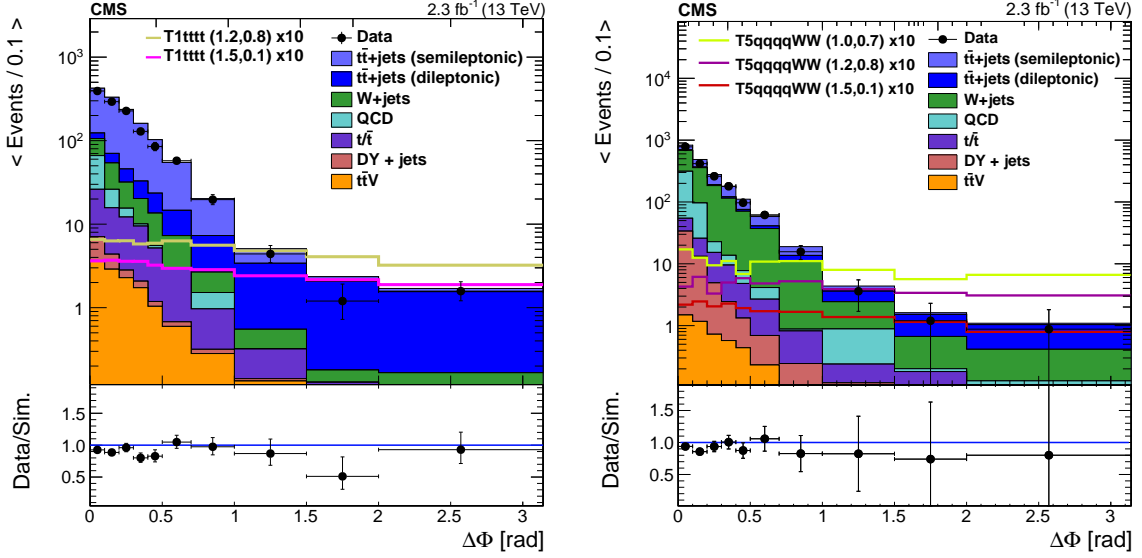


Figure 3: Comparison of the $\Delta\Phi$ distribution for (left) the multi-b and (right) the zero-b analysis after the baseline selection. The simulated background events are stacked on top of each other, and several signal points are overlaid for illustration, but without stacking. The wider bins are normalized to a bin width of 0.1. The label DY refers to $q\bar{q} \rightarrow Z/\gamma^* \rightarrow \ell^+\ell^-$ events, and QCD refers to multijet events. The event yields for the benchmark models have been scaled up by a factor of 10. The ratio of data to simulation is given below each of the panels.

5 Background estimation

The dominant backgrounds in this search are from $t\bar{t}$ +jets and W +jets events, whose contributions vary with the multiplicity of b -tagged jets and the kinematic region in H_T and L_T . To determine these backgrounds, we define two regions for each bin in L_T , H_T , and n_b : the search region (SR) with large values of $\Delta\Phi$, and the control region (CR) with low values of $\Delta\Phi$, with the separation requirement depending on the L_T value, as shown in Table 2. We further divide each of these bins into low- n_{jet} sideband (SB) and high- n_{jet} main band (MB) regions.

About 10–15% of the SM background events in the CR are expected to be multijet events (denoted in the following as QCD), and are predicted as described in Section 5.3. Since the multijet background is negligible in the SR, it is subtracted from the number of background events in the CR when calculating the transfer factor $R_{\text{CS}}^{\text{data}}$ to extrapolate from CR (low- $\Delta\Phi$) to SR (high- $\Delta\Phi$). This transfer factor $R_{\text{CS}}^{\text{data}}$ is determined from data in the low- n_{jet} SB regions, separately for each L_T , H_T , and n_b search region:

$$R_{\text{CS}}^{\text{data}} = \frac{N_{\text{data}}^{\text{SB}}(\text{SR})}{N_{\text{data}}^{\text{SB}}(\text{CR}) - N_{\text{QCD pred}}^{\text{SB}}(\text{CR})}, \quad (1)$$

where $N_{\text{data}}^{\text{SB}}(\text{SR})$ is the number of events in the low- n_{jet} SB high- $\Delta\Phi$ signal region, $N_{\text{data}}^{\text{SB}}(\text{CR})$ the number of events in the low- n_{jet} SB low- $\Delta\Phi$ control region, and $N_{\text{QCD pred}}^{\text{SB}}(\text{CR})$ the predicted number of QCD multijet events in the SB CR.

In the regions with one b tag and four or five jets, about 80% $t\bar{t}$ +jets events and 15–20% W +jets and single top quark events are expected, while in all other multi- b regions, $t\bar{t}$ background is completely dominant. Because only a single SM background dominates in the multi- b analysis, just one R_{CS} factor is needed for each L_T , H_T , and n_b range. In the zero- b bins, the contributions from W +jets and $t\bar{t}$ +jets are roughly equal. Here, an extension of the multi- b strategy is employed, which takes into account differences in the R_{CS} values for these two backgrounds.

An overview of the (n_{jet}, n_b) regions used in this analysis, as discussed in detail in the following Sections 5.1 to 5.3, is given in Table 3.

Table 3: Overview of the definitions of sideband and mainband regions. For the multijet (QCD) fit the electron (e) sample is used, while for the determination (det.) of $R_{\text{CS}}(W^\pm)$ the muon (μ) sample is used. Empty cells are not used in this analysis.

Analysis	Multi-b analysis		Zero-b analysis	
	$n_b = 0$	$n_b \geq 1$	$n_b = 0$	$n_b = 1$
$n_{\text{jet}} = 3$	QCD bkg. fit (e sample)		$R_{\text{CS}}(W^\pm)$ det. (μ sample),	
$n_{\text{jet}} = 4$	QCD bkg. fit (e sample)	R_{CS} det.	QCD bkg. fit (e sample)	$R_{\text{CS}}(\bar{t}\bar{t}+\text{jets})$ det.
$n_{\text{jet}} = 5$		R_{CS} det.	MB	$R_{\text{CS}}(\bar{t}\bar{t}+\text{jets})$ det.
$n_{\text{jet}} \geq 6$		MB	MB	

5.1 Estimate of the leading backgrounds for $n_b \geq 1$

For the multi-b analysis, the SB region, where R_{CS} is determined, is required to have four or five jets, while the MB region must satisfy $n_{\text{jet}} \in [6 - 8]$ or $n_{\text{jet}} \geq 9$. To account for possible differences in this extrapolation from SB to MB as a function of jet multiplicity, we apply multiplicative correction factors κ_{EW} , determined from simulation. The predicted number $N_{\text{pred}}^{\text{MB}}(\text{SR})$ of background events in each MB SR is then given by:

$$N_{\text{pred}}^{\text{MB}}(\text{SR}) = R_{\text{CS}}^{\text{data}} \kappa_{\text{EW}} \left[N_{\text{data}}^{\text{MB}}(\text{CR}) - N_{\text{QCD pred}}^{\text{MB}}(\text{CR}) \right], \quad (2)$$

with

$$\kappa_{\text{EW}} = \frac{R_{\text{CS}}^{\text{MC}}(\text{MB}, \text{EW})}{R_{\text{CS}}^{\text{MC}}(\text{SB}, \text{EW})}. \quad (3)$$

Here $R_{\text{CS}}^{\text{data}}$ is determined from Eq. (1), $N_{\text{data}}^{\text{MB}}(\text{CR})$ is the number of data events in the CR of the MB region, and $N_{\text{QCD pred}}^{\text{MB}}(\text{CR})$ is the predicted number of multijet events in the MB. The label EW refers to all backgrounds other than multijets. The residual difference of the values of R_{CS} between the SB and MB regions is evaluated in simulation as the correction factor κ_{EW} given by Eq. (3), where $R_{\text{CS}}^{\text{MC}}(\text{MB}, \text{EW})$ is the R_{CS} in a search MB region from simulation and $R_{\text{CS}}^{\text{MC}}(\text{SB}, \text{EW})$ is the R_{CS} in the corresponding SB region in simulation for the EW background.

The κ_{EW} factor is determined separately for each search bin, except that an overall κ_{EW} -factor is applied for the $n_b \geq 2$ search bins with the same H_T and L_T , since the κ_{EW} factors are found to be nearly independent of n_b . Similarly, R_{CS} at very high H_T is determined jointly across all three n_b bins to increase the number of events, as the overall uncertainty of the background prediction for several of the search bins is dominated by the statistical uncertainty of the yield in the CR of the main band.

The value of R_{CS} for the total background is equal to the sum of the R_{CS} values of each background component, weighted with the relative contributions of the components. For semileptonic $\bar{t}\bar{t}$ and $W+\text{jets}$ events, which contain both one neutrino from the hard interaction, R_{CS} typically has values of 0.01 to 0.04, depending on the search bin. In events with more than one neutrino, e.g. in $\bar{t}\bar{t}$ events in which both W bosons decay leptonically, R_{CS} is higher with values of around 0.5. This is visible in Fig. 3, where at high $\Delta\Phi$ a large fraction of events is due to dileptonic $\bar{t}\bar{t}+\text{jets}$ background, while the low- $\Delta\Phi$ region is dominated by events with only one neutrino. A larger R_{CS} is also expected for events with three neutrinos, such as $\bar{t}\bar{t}Z$, when the $\bar{t}\bar{t}$ system decays semileptonically and the Z boson decays to two neutrinos. The influence of these latter processes is small, since their relative contribution to the background is minor.

Most of the SRs with six or more jets are dominated by semileptonic $t\bar{t}$ events, and therefore this background dominates the total R_{CS} value of ≈ 0.05 . As the R_{CS} for dileptonic $t\bar{t}$ events is an order of magnitude larger than for semileptonic $t\bar{t}$ events, a slight change in composition in the CR from low- to high- n_{jet} multiplicity translates into κ_{EW} slightly different from unity. This change in the dileptonic $t\bar{t}$ contribution is accounted for by assigning an uncertainty on the n_{jet} extrapolation based on a dileptonic control sample in data, as discussed in Section 6.

5.2 Estimate of the leading backgrounds for $n_b = 0$

For search bins in which b-tagged jets are vetoed, the background contributions from W+jets and $t\bar{t}$ +jets events are estimated by applying the R_{CS} method separately to each of the two components. This strategy implies the use of two sidebands enriched in W+jets and $t\bar{t}$ +jets events, respectively. We write the total background in each search region n_{jet}^{SR} (with a $\Delta\Phi$ requirement as shown in Table 2) as:

$$N_{MB}^{SR}(0b) = N_W^{SR}(0b) + N_{t\bar{t}}^{SR}(0b) + N_{other}^{SR(MC)}(0b), \quad (4)$$

where the predicted yields of W+jets and $t\bar{t}$ +jets background events are denoted by N_W^{SR} and $N_{t\bar{t}}^{SR}$, respectively. Additional backgrounds from rare sources are estimated from simulation and denoted by $N_{other}^{SR(MC)}$.

The expected number of events for each of the background components can be described by:

$$N_i^{SR} = N_{data}^{CR} f_i R_{CS}^i, \quad \text{with } i = [W, t\bar{t}], \quad (5)$$

where N_{data}^{CR} is the total number of events in the CR of the MB region and f_i is the relative yield of component i . The relative contributions of the two components are determined by a fit of templates obtained from simulation to the n_b multiplicity distribution in the CR of the MB region. The contribution of the QCD multijet background in the CR is fixed to the yield estimated from data as described in Section 5.3. The contribution of other rare background components is obtained from simulation as well, as is done in the SR. Uncertainties in these two components are propagated as systematic uncertainties to the final prediction. Examples of these fits are shown in Fig. 4.

The two R_{CS} values, for W+jets and $t\bar{t}$ +jets, are measured in two different low n_{jet} SB regions. For the $t\bar{t}$ +jets estimate a sideband with the requirements $4 \leq n_{jet} \leq 5$ and $n_b = 1$ is used. The value of $R_{CS}^{t\bar{t}}$ is then given by:

$$R_{CS}^{t\bar{t}}(0b, n_{jet}^{SR}) = \kappa_b \kappa_{t\bar{t}} R_{CS}^{data}(1b, n_{jet} \in [4, 5]). \quad (6)$$

The correction factors κ_b and $\kappa_{t\bar{t}}$ are determined from simulation. The factor κ_b corrects for a potential difference of $R_{CS}^{t\bar{t}}$ between samples with zero or one b jet and for the small contributions of backgrounds other than $t\bar{t}$ +jets or QCD multijet events. The factor $\kappa_{t\bar{t}}$ corrects for a residual dependence of $R_{CS}^{t\bar{t}}$ on n_{jet} , in analogy to the κ_{EW} factor defined in Section 5.1. Both values, κ_b and $\kappa_{t\bar{t}}$, are close to unity, and statistical uncertainties from the simulation are propagated to the predicted yields.

Similarly, the W+jets contribution is estimated using R_{CS} values from a sideband with $3 \leq n_{jet} \leq 4$ and $n_b = 0$. With respect to the SB used for the estimate of $R_{CS}^{t\bar{t}}$, a lower jet multiplicity is chosen in order to limit the contamination from $t\bar{t}$ +jets events. Only the muon channel is used since it has a negligible contamination from QCD multijet events, contrary to the electron

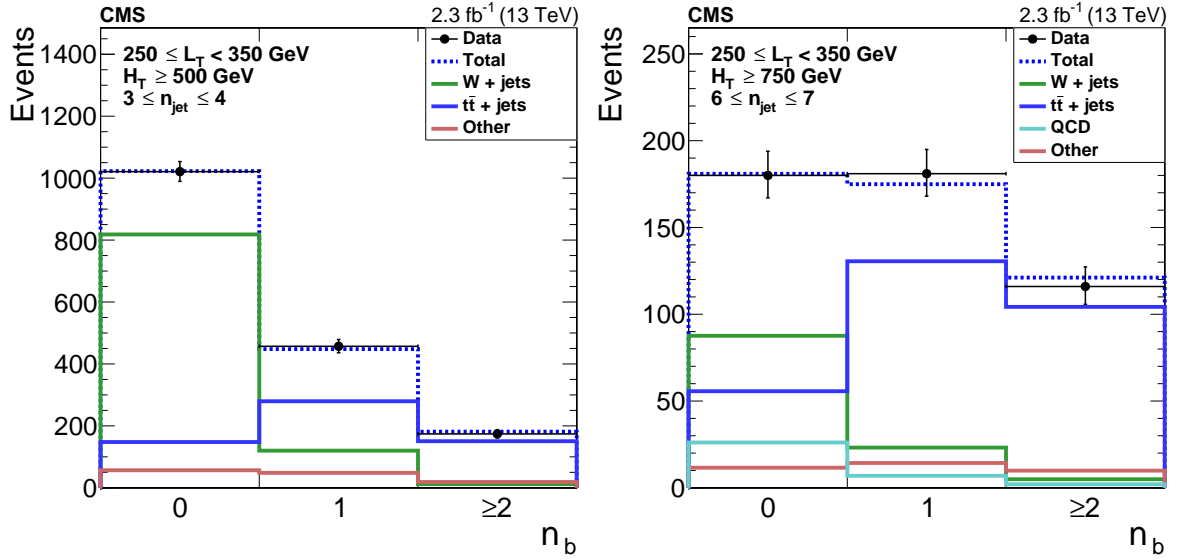


Figure 4: Fits to the n_b multiplicity for control regions in (left) $3 \leq n_{\text{jet}} \leq 4$ ($250 \leq L_T < 350$ GeV, $H_T \geq 500$ GeV, $\Delta\Phi < 1$) and (right) $6 \leq n_{\text{jet}} \leq 7$ ($250 \leq L_T < 350$ GeV, $H_T \geq 750$ GeV, $\Delta\Phi < 1$) in data (muon channel). The solid lines represent the templates scaled according to the fit result (blue for $t\bar{t}$ +jets, green for W+jets, turquoise for QCD, and red for the remaining backgrounds), the dashed line shows the sum after fit, and the points with error bars represent data.

channel. A systematic uncertainty is derived from simulation to cover potential differences between the μ and the combined e and μ samples. The value of R_{CS}^{W} is given by:

$$R_{\text{CS}}^{\text{W}}(0b, n_{\text{jet}}^{\text{SR}}) = \kappa_{\text{W}} R_{\text{CS}}^{\text{data(corr)}}(0b, n_{\text{jet}} \in [3, 4]). \quad (7)$$

Again, the factor κ_{W} corrects for a residual dependence of R_{CS}^{W} on the jet multiplicity. The raw value of $R_{\text{CS}}^{\text{data}}$ measured in the SB has to be corrected for the contamination of $t\bar{t}$ +jets events. The $t\bar{t}$ +jets yields are subtracted in the numerator and denominator according to:

$$R_{\text{CS}}^{\text{data(corr)}}(0b, n_{\text{jet}} \in [3, 4]) = \frac{N_{\text{data}}^{\text{SR}} - R_{\text{CS}}^{\text{t}\bar{\text{t}}, \text{MC}} f_{\text{t}\bar{\text{t}}} N_{\text{data}}^{\text{CR}}}{(1 - f_{\text{t}\bar{\text{t}}}) N_{\text{data}}^{\text{CR}}}. \quad (8)$$

The event yields $N_{\text{data}}^{\text{CR}}$ and $N_{\text{data}}^{\text{SR}}$ are measured in the SB CRs and SRs. The fraction of $t\bar{t}$ +jets events $f_{\text{t}\bar{\text{t}}}$ is again obtained by a fit to the n_b multiplicity in the SB CR. The R_{CS} value for $t\bar{t}$ +jets in this SB is obtained from simulation.

Systematic uncertainties are assigned to $\kappa_{\text{t}\bar{\text{t}}}$ and κ_{W} according to the difference between the R_{CS} values in the sideband and the result of a linear fit over the full range of n_{jet} . The uncertainties vary from 3 to 43% for $\kappa_{\text{t}\bar{\text{t}}}$ and from 1 to 49% for κ_{W} . The two sources are treated as being independent.

5.3 Estimate of the multijet background

Multijet events enter this analysis mostly when reconstructed electrons originate from misidentified jets or from photon conversion in the inner detector. This background is estimated from the yield of ‘antiselected’ electron candidates in each region, that pass looser identification and isolation requirements, and fail the tighter criteria for selected electrons. These events are scaled by the ratio of jets and photons that pass the tight electron identification requirements to the number of antiselected electron candidates in a multijet-enriched control sample with no

b-tagged jets and three or four other jets. The assumption is that this sample is devoid of genuine prompt electrons. The estimation method was introduced previously [10, 52], and relies on the L_P variable:

$$L_P = \frac{p_T^\ell}{p_T^W} \cos(\Delta\Phi). \quad (9)$$

For the dominant SM backgrounds, $t\bar{t}$ +jets and W+jets, the distribution of L_P is a well-understood consequence of the W boson polarization and falls from 0 to 1. In contrast, the distribution of L_P for multijet events peaks near $L_P = 1$.

The ratio of selected to antiselected electron candidates is obtained from a fit to the L_P distribution in bins of L_T . The shape of the QCD multijet contribution used in the fit is taken from the antiselected sample, while the shape of all other contributions is taken from simulation, as the behavior due to W polarization is well understood. The ratios are found to be in the range 0.1–0.2.

In principle, the background estimation with the R_{CS} method requires knowledge of the multijet contribution in the SR and CR separately. Since the multijet background estimation is performed inclusively with respect to $\Delta\Phi$, an R_{CS} factor for multijet events is determined as well. In practice, since the resulting R_{CS} values are all found to be below 2%, the multijet contamination is negligible for the SR. Therefore, the previously described R_{CS} method takes into account only the QCD multijet contribution in the CR, as written in Eq. (1). For the muon channel, the contribution from QCD multijet background is typically of the order of 1% of the total background. To estimate this contribution, a procedure similar to the one outlined above is applied, and assigned a 100% uncertainty.

6 Systematic uncertainties

Systematic uncertainties either influence κ , and thereby the predictions for the background, or modify the expected signal yield.

The main systematic uncertainty on the background arises from the extrapolation of R_{CS} from the low n_{jet} region, where it is measured, to the MB regions of higher jet multiplicities, where it is applied. Therefore, a systematic uncertainty on R_{CS} is determined in a dedicated control region with dileptonic events. The ratio of the semileptonic to dileptonic $t\bar{t}$ +jets final states for different numbers of reconstructed jets is of major importance, since the total R_{CS} is based on the fraction of the two channels and their corresponding R_{CS} values, which differ significantly in $t\bar{t}$ +jets events. To ensure that the data are described well by simulation, a high-purity dilepton $t\bar{t}$ +jets control sample is selected from the data by requiring two leptons of opposite charge. For same-flavor leptons it is also required that the invariant mass of the lepton pair be more than 10 GeV away from the Z boson mass peak. To study the behavior of the dileptonic events in the single-lepton selection, one of the two leptons is removed from the event. Since these “lost leptons” are principally from $\tau \rightarrow \text{hadrons} + \nu$ decays, we replace the removed lepton by a jet with 2/3 of the original lepton’s p_T to accommodate for the missing energy due to the neutrino from the τ decay, and recalculate the L_T , $\Delta\Phi$, and H_T values of the now “single-lepton” event. In order to maximize the number of events, no $\Delta\Phi$ requirement is applied, and all events are used twice, with each reconstructed lepton being considered as the lost lepton. We refer to the samples produced using this procedure as the dilepton CRs.

A key test is performed by comparing the jet multiplicity distribution in the sample resulting from single-lepton baseline selection (excluding the SRs) with the corresponding simulated event sample, and by comparing the dilepton CRs with the corresponding simulated event

sample. Both comparisons show the same trend, a slight overprediction by simulation of the rate of high jet multiplicity events. The ratio of event yields in data-to-simulation is computed for each comparison and the two ratios are then divided to see whether the behavior in data relative to simulation is the same in both pairs of samples. This double ratio is consistent with unity within statistical uncertainty. The systematic uncertainty in the description of the n_{jet} distribution in simulation is determined from this double ratio, and is mainly due to the statistical uncertainty of the data samples, which is within 8–40%, and therefore larger than the observed slope of the double ratio vs. n_{jet} .

The remaining uncertainties are smaller than the one from the dileptonic $t\bar{t}$ +jets fraction. In particular, the applied jet energy scale (JES) factors are varied up and down according to their uncertainty [25] as a function of jet p_T and η , and these changes are propagated to E_T^{miss} . The scale factors applied to the efficiencies for the identification of b-quark jets and for the misidentification of c-quark, light-quark or gluon jets are also varied up and down according to their uncertainties [34]. Uncertainties for the efficiency of lepton reconstruction and identification are handled in the same way. For pileup, a 5% uncertainty in the inelastic cross section [53] is used to obtain its impact on the uncertainty in the pileup. In a few bins with low number of simulated events, the reweighting leads to a large uncertainty. All these uncertainties apply to both the background prediction and the signal yield. The luminosity is measured with the pixel cluster counting method, and the absolute luminosity scale calibration is derived from an analysis of Van der Meer scans performed in August 2015, resulting in an uncertainty of 2.7% [54].

The W+jets and $t\bar{t}$ +jets cross sections are changed by 30% [55] to cover possible biases in the estimation of the background composition in terms of W+jets vs. $t\bar{t}$ +jets events, which would lead to a slight change in the κ value. These changes have only a small impact on the zero-b analysis, where the relative fraction of the two processes is determined from a fit. Also, the following changes in the simulation are performed, with differences between the values of κ in the reweighted and original samples defining the uncertainties. Motivated by measurements at $\sqrt{s} = 8$ TeV, simulated $t\bar{t}$ +jets events are reweighted by a factor $\sqrt{F(p_T^t) F(p_T^{\bar{t}})}$, with $F(p_T^t) = \min(0.5, \exp(0.156 - 0.00137 p_T^t))$, to improve the modelling of the top quark p_T spectrum [56]. The reweighting preserves the normalization of the sample, and the difference relative to the results obtained with the unweighted sample is assigned as a systematic uncertainty. The polarization of W bosons is varied by reweighting events by the factor $w(\cos\theta^*) = 1 + \alpha(1 - \cos\theta^*)^2$, where θ^* is the angle between the charged lepton and W boson in the W boson rest frame. In W+jets events, we take α to be 0.1, guided by the theoretical uncertainty and measurements found in Refs. [52, 57–59]. For $t\bar{t}$ +jets events, we take $\alpha = 0.05$. For W+jets events, where the initial state can have different polarizations for W^+ vs. W^- bosons, we take as uncertainty the larger change in κ resulting from reweighting only the W^+ bosons in the sample, and from reweighting all W bosons. The $t\bar{t}V$ cross section is varied by 100%. The systematic uncertainty in the multijet estimation depends on n_{jet} and n_b , and ranges from 25% to 100%.

For the zero-b analysis, an additional systematic uncertainty is applied, based on linear fits of R_{CS} as a function of n_{jet} as described in Section 5.2, and a 50% cross section uncertainty is used for all backgrounds other than W+jets, $t\bar{t}$ +jets, $t\bar{t}V$, and multijets.

For the signal, an uncertainty in initial-state radiation (ISR) is applied, based on the p_T of the gluino-gluino system, which corresponds to a 15% uncertainty at p_T between 400 and 600 GeV, and 30% at larger p_T . This uncertainty is based on measurements of ISR in Z+jets and $t\bar{t}$ +jets events [16, 60]. The factorization and renormalization scale are each changed by a factor of 0.5

and 2. Uncertainties in the signal cross section are also taken into account.

The impact of the systematic uncertainties in the total background prediction for the multi-b and zero-b analyses are summarized in Table 4. While the systematic uncertainty is determined for each signal point, the uncertainties typical for most signals are summarized for illustration in Table 5.

Table 4: Summary of systematic uncertainties in the total background prediction for the multi-b and for the zero-b analysis.

Source	Uncertainty for multi-b [%]	Uncertainty for zero-b [%]
Dilepton control sample	5.8–20	7.5–40
JES	0.2–11	0.6–8.2
Tagging of b-jets	0.1–17	1.4–4.5
$\sigma(W+\text{jets})$	0.3–6.4	<2.5
W polarization	0.1–2	0.2–3.4
$\sigma(t\bar{t}V)$	0.1–5	0.2–2.9
Reweighting of top quark p_T	0.1–10	0.1–7.1
Pileup	0.3–23	0.1–10
Fit to $R_{CS}(n_{\text{jet}})$ ($W+\text{jets}$ and $t\bar{t}+\text{jets}$)	—	3.3–35
Total	8.0–28	10–54
Statistical uncertainty in MC events	3.0–30	8.2–48

Table 5: Summary of the systematic uncertainties and their average effect on the yields of the benchmark signals. The values are very similar for the multi-b and the zero-b analysis, and are usually larger for compressed scenarios, where the mass difference between gluino and neutralino is small.

Source	Uncertainty [%]
Trigger	1
Pileup	5
Lepton efficiency	5
Luminosity	2.7
ISR	3–20
Tagging of b-jets (heavy flavors)	6–10
Tagging of b-jets (light flavors)	2–3
JES	3–10
Factorization/renormalization scale	< 3
Total	12–26

7 Results and interpretation

The backgrounds for all SRs are determined, as described previously, in different SB regions with lower jet or b-jet multiplicities. The result of the background prediction and the observed data are shown in Table 6 and Fig. 5 for the multi-b events. In this figure, the outline of the filled histogram represents the total number of background events from the prediction. For illustration, the relative amount of $t\bar{t}+\text{jets}$, $W+\text{jets}$, and of other backgrounds is shown as well, based on the fractions estimated in simulation. Table 7 and Fig. 6 show the results for the zero-b events. Here, the filled histogram represents the predictions from data for $t\bar{t}+\text{jets}$ and $W+\text{jets}$ events, and for the remaining backgrounds, where the latter include the multijet prediction

determined from data and rare backgrounds taken from simulation. The data agree with SM expectations and no excess is observed.

Table 6: Summary of the results in the multi-b search.

n_{jet}	L_T [GeV]	H_T [GeV]	n_b	Bin name	Expected signal T1tttt $m_{\tilde{g}}/m_{\tilde{\chi}_1^0}$ [TeV]		Predicted background	Observed
					(1.5,0.1)	(1.2,0.8)		
[6, 8]	[250, 350]	[500, 750]	= 1	LT1, HT0, NB1	< 0.01	0.41 ± 0.02	9.0 ± 2.1	9
			= 2	LT1, HT0, NB2	< 0.01	0.67 ± 0.03	8.4 ± 2.1	2
			≥ 3	LT1, HT0, NB3i	< 0.01	0.67 ± 0.03	1.23 ± 0.39	1
		≥ 750	= 1	LT1, HT1i, NB1	0.03 ± 0.00	0.15 ± 0.01	9.8 ± 3.0	14
			= 2	LT1, HT1i, NB2	0.07 ± 0.00	0.27 ± 0.02	7.1 ± 2.7	6
			≥ 3	LT1, HT1i, NB3i	0.07 ± 0.00	0.22 ± 0.02	0.85 ± 0.40	1
	[350, 450]	[500, 750]	= 1	LT2, HT0, NB1	< 0.01	0.19 ± 0.02	2.42 ± 0.96	4
			= 2	LT2, HT0, NB2	0.01 ± 0.00	0.28 ± 0.02	0.89 ± 0.56	2
			≥ 3	LT2, HT0, NB3i	0.01 ± 0.00	0.24 ± 0.02	0.10 ± 0.08	0
		≥ 750	= 1	LT2, HT1i, NB1	0.08 ± 0.00	0.16 ± 0.01	3.6 ± 1.8	5
			= 2	LT2, HT1i, NB2	0.12 ± 0.01	0.24 ± 0.02	3.8 ± 1.9	2
			≥ 3	LT2, HT1i, NB3i	0.13 ± 0.01	0.19 ± 0.01	0.54 ± 0.35	0
[450, 600]	[500, 1250]	= 1	LT3, HT0i, NB1	0.07 ± 0.00	0.18 ± 0.02	4.1 ± 1.6	1	
		≥ 2	LT3, HT0i, NB2i	0.19 ± 0.01	0.42 ± 0.02	4.0 ± 2.1	0	
		≥ 3	LT3, HT0i, NB3i	0.08 ± 0.00	0.02 ± 0.00	0.62 ± 0.69	1	
	≥ 1250	= 1	LT3, HT2i, NB1	0.08 ± 0.00	0.02 ± 0.00	0.62 ± 0.69	1	
		≥ 2	LT3, HT2i, NB2i	0.29 ± 0.01	0.08 ± 0.01	0.59 ± 0.66	1	
		≥ 3	LT3, HT2i, NB3i	0.08 ± 0.00	0.02 ± 0.00	0.62 ± 0.69	1	
≥ 600	[500, 1250]	= 1	LT4i, HT0i, NB1	0.18 ± 0.01	0.05 ± 0.01	0.60 ± 0.51	0	
		≥ 2	LT4i, HT0i, NB2i	0.57 ± 0.01	0.16 ± 0.01	0.25 ± 0.39	0	
		≥ 3	LT4i, HT0i, NB3i	0.26 ± 0.01	0.07 ± 0.01	0.20 ± 0.27	0	
	≥ 1250	= 1	LT4i, HT2i, NB1	0.26 ± 0.01	0.07 ± 0.01	0.20 ± 0.27	0	
		≥ 2	LT4i, HT2i, NB2i	0.95 ± 0.02	0.16 ± 0.01	0.42 ± 0.53	0	
		≥ 3	LT4i, HT2i, NB3i	0.26 ± 0.01	0.07 ± 0.01	0.20 ± 0.27	0	
≥ 9	[250, 350]	[500, 1250]	= 1	LT1, HT0i, NB1	0.01 ± 0.00	0.22 ± 0.02	0.52 ± 0.19	0
			= 2	LT1, HT0i, NB2	0.01 ± 0.00	0.55 ± 0.03	0.23 ± 0.14	0
			≥ 3	LT1, HT0i, NB3i	0.08 ± 0.00	0.74 ± 0.03	0.32 ± 0.16	0
		≥ 500	= 1	LT1, HT2i, NB1	0.02 ± 0.00	0.02 ± 0.01	0.17 ± 0.16	0
			= 2	LT1, HT2i, NB2	0.04 ± 0.00	0.05 ± 0.01	0.24 ± 0.31	0
			≥ 3	LT1, HT2i, NB3i	0.04 ± 0.00	0.05 ± 0.01	0.24 ± 0.31	0
	[350, 450]	≥ 500	= 1	LT2, HT0i, NB1	0.04 ± 0.00	0.23 ± 0.02	0.28 ± 0.14	0
			= 2	LT2, HT0i, NB2	0.10 ± 0.01	0.41 ± 0.02	0.05 ± 0.06	1
			≥ 3	LT2, HT0i, NB3i	0.12 ± 0.01	0.51 ± 0.02	0.04 ± 0.05	0
		≥ 450	= 1	LT3i, HT0i, NB1	0.29 ± 0.01	0.23 ± 0.02	0.31 ± 0.20	0
			≥ 2	LT3i, HT0i, NB2i	1.42 ± 0.02	0.99 ± 0.03	0.15 ± 0.13	0
			≥ 3	LT3i, HT0i, NB3i	0.29 ± 0.01	0.23 ± 0.02	0.31 ± 0.20	0

To set limits, separate likelihood functions, one for the multi-b analysis and one for the zero-b analysis, are constructed from the Poisson probability functions for all four data regions (the CRs and SRs in the SB as well in the MB) to determine the background in the MB SR. In addition, the κ values from simulation are included to correct any residual differences between the SB and MB regions, with uncertainties incorporated through log-normal constraints. The estimated contribution from multijet events in the two CRs is also included. A possible signal contamination is taken into account by including signal terms in the fit for both the sideband and the control regions. For the zero-b analysis, the relative contributions of W +jets and $t\bar{t}$ +jets events as determined in the fits to the n_b distribution in the CRs are treated as external measurements. The correlation between the W +jets and $t\bar{t}$ +jets yields introduced by these fits is taken into account. A profile likelihood ratio in the asymptotic approximation [61] is used as the test statistic. Limits are then calculated at the 95% confidence level (CL) using the asymptotic CL_s criterion [62, 63].

The cross section limits obtained for the T1tttt model using the multi-b analysis, and for the T5qqqqWW model using the zero-b analysis, are shown in Fig. 7 as a function of $m(\tilde{g})$ and $m(\tilde{\chi}_1^0)$, assuming branching fractions of 100% as shown in Fig. 1. Using the $\tilde{g}\tilde{g}$ pair production cross section calculated at next-to-leading order within next-to-leading-logarithmic accuracy, exclusion limits are set as a function of the $(m_{\tilde{g}}, m_{\tilde{\chi}_1^0})$ mass hypothesis.

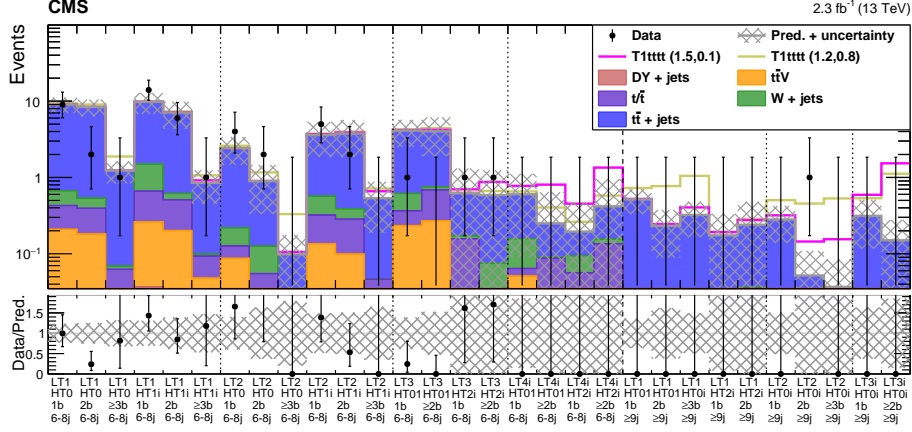


Figure 5: Multi-b search: comparison of observed and predicted background event yields in the 30 search regions. Upper panel: the data are shown by black points with error bars, while the total SM background predictions are shown by a grey line with a hatched region representing its uncertainty. For illustration, the relative fraction of the different SM background contributions, as determined from simulation, is shown by the stacked, colored histograms, whose total normalization is set by the total background yields obtained from the control samples in the data. The expected event yields for two T1tttt SUSY benchmark models are shown by open histograms, each of which is shown stacked on the total background prediction. The vertical dashed and dotted lines separate different n_{jet} and L_T bins, respectively, as indicated by the x -axis labels. Lower panel: the ratio of the yield observed in data to the predicted background yield is shown for each bin. The error bars on the data points indicate the combined statistical and systematic uncertainty in the ratio. The grey hatched region indicates the uncertainty on the ratio that arises from the uncertainty on the background prediction.

Table 7: Summary of the results of the zero-b search.

n_{jet}	L_T [GeV]	H_T [GeV]	Bin name	Expected signal T5qqqWW $m_{\tilde{g}}/m_{\tilde{\chi}^0}$ [TeV]			Predicted background	Observed
				(1.0,0.7)	(1.2,0.8)	(1.5,0.1)		
5	[250, 350]	≥ 500	LT1, HTi	1.67 ± 0.27	0.68 ± 0.07	0.03 ± 0.01	12.8 ± 2.9	13
	[350, 450]	≥ 500	LT2, HTi	1.13 ± 0.22	0.68 ± 0.07	0.04 ± 0.01	4.5 ± 2.2	4
	≥ 450	≥ 500	LT3, HTi	1.48 ± 0.26	0.79 ± 0.08	0.51 ± 0.02	3.9 ± 2.0	1
[6,7]	[250, 350]	[500, 750]	LT1, HT1	3.03 ± 0.36	1.06 ± 0.09	< 0.01	4.2 ± 1.4	8
		≥ 750	LT1, HT23	0.92 ± 0.20	0.36 ± 0.05	0.08 ± 0.01	4.8 ± 1.6	4
	[350, 450]	[500, 750]	LT2, HT1	1.54 ± 0.26	0.90 ± 0.08	< 0.01	1.4 ± 1.1	0
		≥ 750	LT2, HT23	1.15 ± 0.21	0.41 ± 0.05	0.13 ± 0.01	1.29 ± 0.74	2
	≥ 450	[500, 1000]	LT3, HT12	1.99 ± 0.29	1.83 ± 0.12	0.11 ± 0.01	2.25 ± 0.93	0
		≥ 1000	LT3, HT3	1.33 ± 0.23	0.55 ± 0.06	1.38 ± 0.04	1.5 ± 1.0	2
≥ 8	[250, 350]	[500, 750]	LT1, HT1	0.90 ± 0.20	0.26 ± 0.04	< 0.01	0.34 ± 0.22	0
		≥ 750	LT1, HT23	0.85 ± 0.19	0.41 ± 0.05	0.06 ± 0.01	1.10 ± 0.61	1
	[350, 450]	≥ 500	LT2, HTi	1.41 ± 0.23	0.75 ± 0.07	0.09 ± 0.01	0.45 ± 0.28	0
	≥ 450	≥ 500	LT3, HTi	2.44 ± 0.31	1.27 ± 0.09	0.84 ± 0.03	0.39 ± 0.26	0

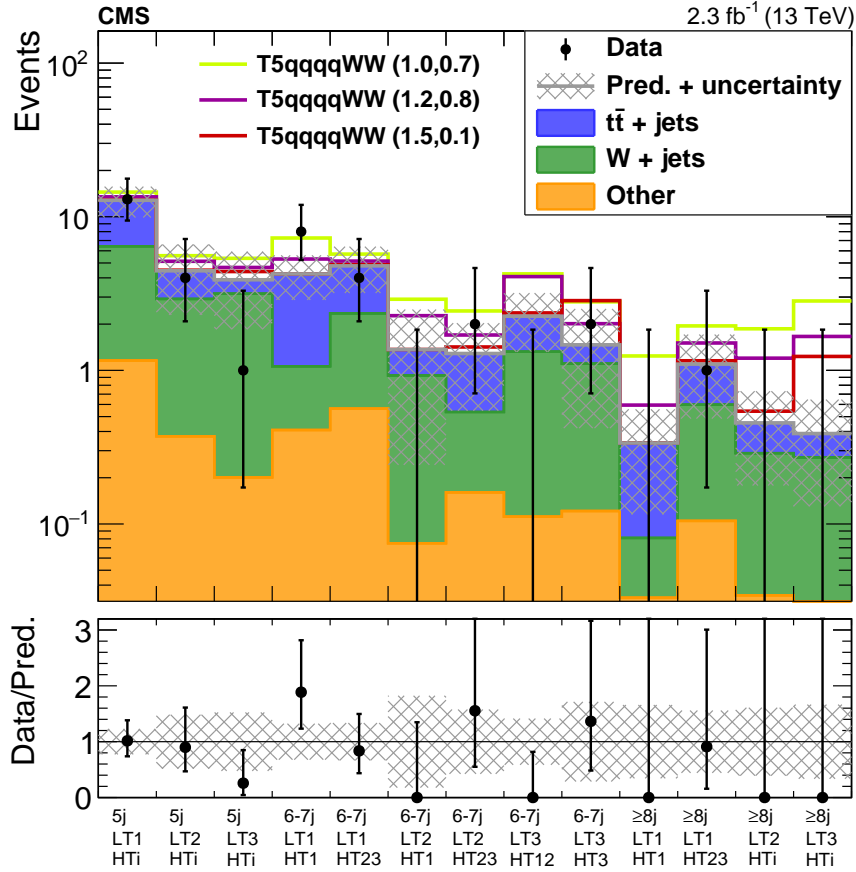


Figure 6: Zero-b search: observed and predicted event counts in the 13 search regions. Upper panel: the black points with error bars show the number of observed events. The filled, stacked histograms represent the predictions for $t\bar{t}$ +jets, W+jets events, and the remaining backgrounds. The uncertainty on the background prediction is shown as a grey, hatched region. The expected yields from three T5qqqqWW model points, added to the SM background, are shown as solid lines. Lower panel: the ratio of the yield observed in data to the predicted background yield is shown for each bin. The error bars on the data points indicate the combined statistical and systematic uncertainty in the ratio. The grey hatched region indicates the uncertainty on the ratio that arises from the uncertainty on the background prediction.

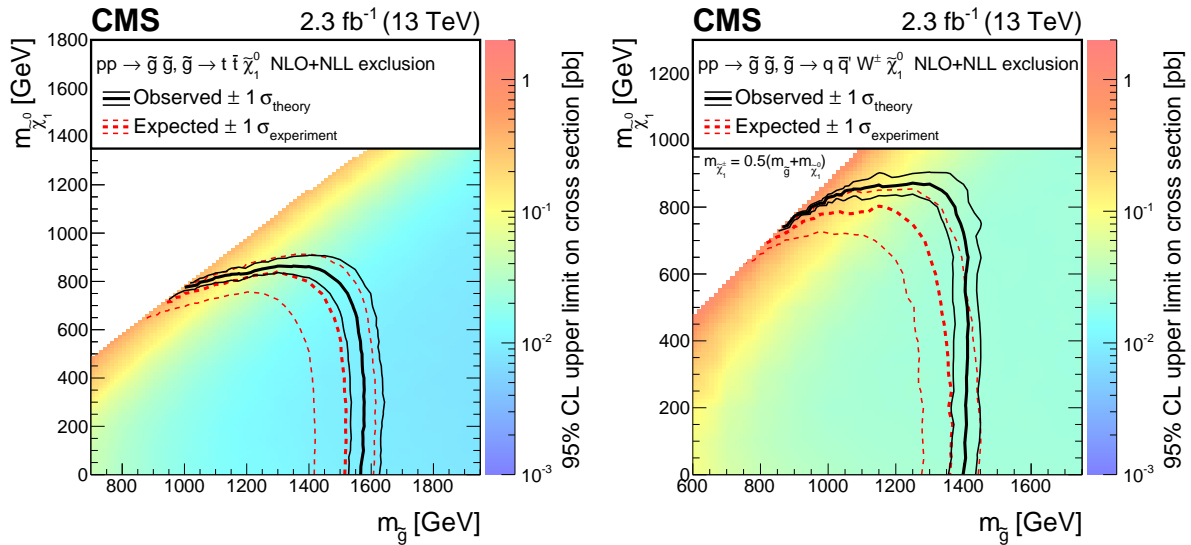


Figure 7: Cross section limits at a 95% CL for the (left) T1tttt and (right) T5qqqWW models, as a function of the gluino and LSP masses. In T5qqqWW, the pair-produced gluinos each decay to a quark-antiquark pair of the first or second generation ($q\bar{q}$), and a chargino ($\tilde{\chi}_1^\pm$) with its mass taken to be $m_{\tilde{\chi}_1^\pm} = 0.5(m_{\tilde{g}} + m_{\tilde{\chi}_1^0})$. The solid black (dashed red) lines correspond to the observed (expected) mass limits, with the thicker lines representing the central values and the thinner lines representing the $\pm 1\sigma$ uncertainty bands related to the theoretical (experimental) uncertainties.

8 Summary

A search for supersymmetry has been performed with 2.3 fb^{-1} of proton-proton collision data recorded by the CMS experiment at $\sqrt{s} = 13 \text{ TeV}$ in 2015. The data are analyzed in several exclusive categories, differing in the number of jets and b-tagged jets, the scalar sum of all jet transverse momenta, and the scalar sum of the missing transverse momentum and the transverse momentum of the lepton. The main background is significantly reduced by requiring a large azimuthal angle between the directions of the momenta of the lepton and of the reconstructed W boson. No significant excess is observed, and the results are interpreted in terms of two simplified models that describe gluino pair production.

For the simplified model T1tttt, in which each gluino decays through an off-shell top squark to a $t\bar{t}$ pair and the lightest neutralino, gluino masses up to 1.6 TeV are excluded for neutralino masses below 600 GeV. Neutralino masses below 850 GeV can be excluded for a gluino mass up to 1.4 TeV. Similar to Ref. [16], these results extend the limits obtained from the 8 TeV searches [13–15] by about 250 GeV.

The second simplified model T5qqqWW also contains gluino pair production, with the gluinos decaying to first or second generation squarks and a chargino, which then decays to a W boson and the lightest neutralino. The chargino mass in this decay chain is taken to be $m_{\tilde{\chi}_1^\pm} = 0.5(m_{\tilde{g}} + m_{\tilde{\chi}_1^0})$. In this model, gluino masses below 1.4 TeV are excluded for neutralino masses below 700 GeV. For a gluino mass of 1.3 TeV, neutralinos with masses up to 850 GeV can be excluded. These results improve existing limits [17] on the neutralino mass in this channel for gluino masses between 900 GeV and 1.4 TeV.

Acknowledgments

We congratulate our colleagues in the CERN accelerator departments for the excellent performance of the LHC and thank the technical and administrative staffs at CERN and at other CMS institutes for their contributions to the success of the CMS effort. In addition, we gratefully acknowledge the computing centers and personnel of the Worldwide LHC Computing Grid for delivering so effectively the computing infrastructure essential to our analyses. Finally, we acknowledge the enduring support for the construction and operation of the LHC and the CMS detector provided by the following funding agencies: BMWFW and FWF (Austria); FNRS and FWO (Belgium); CNPq, CAPES, FAPERJ, and FAPESP (Brazil); MES (Bulgaria); CERN; CAS, MoST, and NSFC (China); COLCIENCIAS (Colombia); MSES and CSF (Croatia); RPF (Cyprus); SENESCYT (Ecuador); MoER, ERC IUT and ERDF (Estonia); Academy of Finland, MEC, and HIP (Finland); CEA and CNRS/IN2P3 (France); BMBF, DFG, and HGF (Germany); GSRT (Greece); OTKA and NIH (Hungary); DAE and DST (India); IPM (Iran); SFI (Ireland); INFN (Italy); MSIP and NRF (Republic of Korea); LAS (Lithuania); MOE and UM (Malaysia); BUAP, CINVESTAV, CONACYT, LNS, SEP, and UASLP-FAI (Mexico); MBIE (New Zealand); PAEC (Pakistan); MSHE and NSC (Poland); FCT (Portugal); JINR (Dubna); MON, RosAtom, RAS and RFBR (Russia); MESTD (Serbia); SEIDI and CPAN (Spain); Swiss Funding Agencies (Switzerland); MST (Taipei); ThEPCenter, IPST, STAR and NSTDA (Thailand); TUBITAK and TAEK (Turkey); NASU and SFFR (Ukraine); STFC (United Kingdom); DOE and NSF (USA).

Individuals have received support from the Marie-Curie program and the European Research Council and EPLANET (European Union); the Leventis Foundation; the A. P. Sloan Foundation; the Alexander von Humboldt Foundation; the Belgian Federal Science Policy Office; the Fonds pour la Formation à la Recherche dans l'Industrie et dans l'Agriculture (FRIA-Belgium); the Agentschap voor Innovatie door Wetenschap en Technologie (IWT-Belgium); the Ministry of Education, Youth and Sports (MEYS) of the Czech Republic; the Council of Science and Industrial Research, India; the HOMING PLUS program of the Foundation for Polish Science, cofinanced from European Union, Regional Development Fund, the Mobility Plus program of the Ministry of Science and Higher Education, the National Science Center (Poland), contracts Harmonia 2014/14/M/ST2/00428, Opus 2013/11/B/ST2/04202, 2014/13/B/ST2/02543 and 2014/15/B/ST2/03998, Sonata-bis 2012/07/E/ST2/01406; the Thalys and Aristeia programs cofinanced by EU-ESF and the Greek NSRF; the National Priorities Research Program by Qatar National Research Fund; the Programa Clarín-COFUND del Principado de Asturias; the Rachadapisek Sompot Fund for Postdoctoral Fellowship, Chulalongkorn University and the Chulalongkorn Academic into Its 2nd Century Project Advancement Project (Thailand); and the Welch Foundation, contract C-1845.

References

- [1] P. Ramond, “Dual theory for free fermions”, *Phys. Rev. D* **3** (1971) 2415, doi:10.1103/PhysRevD.3.2415.
- [2] Y. A. Golfand and E. P. Likhtman, “Extension of the algebra of Poincaré group generators and violation of P invariance”, *JETP Lett.* **13** (1971) 323.
- [3] A. Neveu and J. H. Schwarz, “Factorizable dual model of pions”, *Nucl. Phys. B* **31** (1971) 86, doi:10.1016/0550-3213(71)90448-2.
- [4] D. V. Volkov and V. P. Akulov, “Possible universal neutrino interaction”, *JETP Lett.* **16** (1972) 438.
- [5] J. Wess and B. Zumino, “A Lagrangian model invariant under supergauge transformations”, *Phys. Lett. B* **49** (1974) 52, doi:10.1016/0370-2693(74)90578-4.
- [6] J. Wess and B. Zumino, “Supergauge transformations in four dimensions”, *Nucl. Phys. B* **70** (1974) 39, doi:10.1016/0550-3213(74)90355-1.
- [7] P. Fayet, “Supergauge invariant extension of the Higgs mechanism and a model for the electron and its neutrino”, *Nucl. Phys. B* **90** (1975) 104, doi:10.1016/0550-3213(75)90636-7.
- [8] H. P. Nilles, “Supersymmetry, supergravity and particle physics”, *Phys. Rep.* **110** (1984) 1, doi:10.1016/0370-1573(84)90008-5.
- [9] G. R. Farrar and P. Fayet, “Phenomenology of the production, decay, and detection of new hadronic states associated with supersymmetry”, *Phys. Lett. B* **76** (1978) 575, doi:10.1016/0370-2693(78)90858-4.
- [10] CMS Collaboration, “Search for supersymmetry in pp collisions at $\sqrt{s} = 7$ TeV in events with a single lepton, jets, and missing transverse momentum”, *Eur. Phys. J. C* **73** (2013) 2404, doi:10.1140/epjc/s10052-013-2404-z, arXiv:1212.6428.
- [11] CMS Collaboration, “Search for supersymmetry in final states with a single lepton, b-quark jets, and missing transverse energy in proton-proton collisions at $\sqrt{s} = 7$ TeV”, *Phys. Rev. D* **87** (2013) 052006, doi:10.1103/PhysRevD.87.052006, arXiv:1211.3143.
- [12] ATLAS Collaboration, “Further search for supersymmetry at $\sqrt{s} = 7$ TeV in final states with jets, missing transverse momentum and isolated leptons with the ATLAS detector”, *Phys. Rev. D* **86** (2012) 092002, doi:10.1103/PhysRevD.86.092002, arXiv:1208.4688.
- [13] CMS Collaboration, “Search for supersymmetry in pp collisions at $\sqrt{s} = 8$ TeV in events with a single lepton, large jet multiplicity, and multiple b jets”, *Phys. Lett. B* **733** (2014) 328, doi:10.1016/j.physletb.2014.04.023, arXiv:1311.4937.
- [14] ATLAS Collaboration, “Search for squarks and gluinos in events with isolated leptons, jets and missing transverse momentum at $\sqrt{s} = 8$ TeV with the ATLAS detector”, *JHEP* **04** (2015) 116, doi:10.1007/JHEP04(2015)116, arXiv:1501.03555.

- [15] ATLAS Collaboration, “Search for strong production of supersymmetric particles in final states with missing transverse momentum and at least three b-jets at $\sqrt{s} = 8$ TeV proton-proton collisions with the ATLAS detector”, *JHEP* **10** (2014) 024, doi:10.1007/JHEP10(2014)024, arXiv:1407.0600.
- [16] CMS Collaboration, “Search for supersymmetry in pp collisions at $\sqrt{s} = 13$ TeV in the single-lepton final state using the sum of masses of large-radius jets”, *JHEP* **08** (2016) 122, doi:10.1007/JHEP08(2016)122, arXiv:1605.04608.
- [17] ATLAS Collaboration, “Search for gluinos in events with an isolated lepton, jets and missing transverse momentum at $\sqrt{s} = 13$ TeV with the ATLAS detector”, (2016). arXiv:1605.04285. Submitted to *EPJC*.
- [18] ATLAS Collaboration, “Search for pair production of gluinos decaying via stop and sbottom in events with b-jets and large missing transverse momentum in pp collisions at $\sqrt{s} = 13$ TeV with the ATLAS detector”, (2016). arXiv:1605.09318.
- [19] N. Arkani-Hamed et al., “MARMOSSET: The path from LHC data to the new standard model via on-shell effective theories”, (2007). arXiv:hep-ph/0703088.
- [20] J. Alwall, P. C. Schuster, and N. Toro, “Simplified models for a first characterization of new physics at the LHC”, *Phys. Rev. D* **79** (2009) 075020, doi:10.1103/PhysRevD.79.075020, arXiv:0810.3921.
- [21] J. Alwall, M.-P. Le, M. Lisanti, and J. G. Wacker, “Model-independent jets plus missing energy searches”, *Phys. Rev. D* **79** (2009) 015005, doi:10.1103/PhysRevD.79.015005, arXiv:0809.3264.
- [22] D. Alves et al., “Simplified models for LHC new physics searches”, *J. Phys. G* **39** (2012) 105005, doi:10.1088/0954-3899/39/10/105005, arXiv:1105.2838.
- [23] CMS Collaboration, “The CMS experiment at the CERN LHC”, *JINST* **3** (2008) S08004, doi:10.1088/1748-0221/3/08/S08004.
- [24] CMS Collaboration, “Description and performance of track and primary-vertex reconstruction with the CMS tracker”, *JINST* **9** (2014) P10009, doi:10.1088/1748-0221/9/10/P10009, arXiv:1405.6569.
- [25] CMS Collaboration, “Determination of jet energy calibration and transverse momentum resolution in CMS”, *JINST* **6** (2011) P11002, doi:10.1088/1748-0221/6/11/P11002, arXiv:1107.4277.
- [26] CMS Collaboration, “Performance of electron reconstruction and selection with the CMS detector in proton-proton collisions at $\sqrt{s} = 8$ TeV”, *JINST* **10** (2015) P06005, doi:10.1088/1748-0221/10/06/P06005, arXiv:1502.02701.
- [27] CMS Collaboration, “Performance of CMS muon reconstruction in pp collision events at $\sqrt{s} = 7$ TeV”, *JINST* **7** (2012) P10002, doi:10.1088/1748-0221/7/10/P10002, arXiv:1206.4071.
- [28] CMS Collaboration, “Particle-flow event reconstruction in CMS and performance for jets, taus, and E_T^{miss} ”, CMS Physics Analysis Summary CMS-PAS-PFT-09-001, CERN, 2009.

- [29] CMS Collaboration, “Commissioning of the particle-flow event with the first LHC collisions recorded in the CMS detector”, CMS Physics Analysis Summary CMS-PAS-PFT-10-001, CERN, 2010.
- [30] M. Cacciari, G. P. Salam, and G. Soyez, “The Anti-k(t) jet clustering algorithm”, *JHEP* **04** (2008) 063, doi:10.1088/1126-6708/2008/04/063, arXiv:0802.1189.
- [31] M. Cacciari, G. P. Salam, and G. Soyez, “FastJet User Manual”, *Eur. Phys. J.* **C72** (2012) 1896, doi:10.1140/epjc/s10052-012-1896-2, arXiv:1111.6097.
- [32] M. Cacciari and G. P. Salam, “Pileup subtraction using jet areas”, *Phys. Lett. B* **659** (2008) 119, doi:10.1016/j.physletb.2007.09.077, arXiv:0707.1378.
- [33] CMS Collaboration, “Identification of b-quark jets with the CMS experiment”, *JINST* **8** (2013) P04013, doi:10.1088/1748-0221/8/04/P04013, arXiv:1211.4462.
- [34] CMS Collaboration, “Identification of b quark jets at the CMS Experiment in the LHC Run 2”, CMS Physics Analysis Summary CMS-PAS-BTV-15-001, CERN, 2016.
- [35] CMS Collaboration, “Performance of b tagging at $\sqrt{s} = 8$ TeV in multijet, $t\bar{t}$ and boosted topology events”, CMS Physics Analysis Summary CMS-PAS-BTV-13-001, CERN, 2013.
- [36] J. Alwall et al., “MadGraph5: going beyond”, *JHEP* **06** (2011) 128, doi:10.1007/JHEP06(2011)128, arXiv:1106.0522.
- [37] NNPDF Collaboration, “Parton distributions for the LHC Run II”, *JHEP* **04** (2015) 040, doi:10.1007/JHEP04(2015)040, arXiv:1410.8849.
- [38] P. Nason, “A new method for combining NLO QCD with shower Monte Carlo algorithms”, *JHEP* **11** (2004) 040, doi:10.1088/1126-6708/2004/11/040, arXiv:hep-ph/0409146.
- [39] S. Frixione, P. Nason, and C. Oleari, “Matching NLO QCD computations with parton shower simulations: the POWHEG method”, *JHEP* **11** (2007) 070, doi:10.1088/1126-6708/2007/11/070, arXiv:0709.2092.
- [40] S. Alioli, P. Nason, C. Oleari, and E. Re, “A general framework for implementing NLO calculations in shower Monte Carlo programs: the POWHEG BOX”, *JHEP* **06** (2010) 043, doi:10.1007/JHEP06(2010)043, arXiv:1002.2581.
- [41] S. Alioli, P. Nason, C. Oleari, and E. Re, “NLO single-top production matched with shower in POWHEG: s- and t-channel contributions”, *JHEP* **09** (2009) 111, doi:10.1088/1126-6708/2009/09/111, arXiv:0907.4076. [Erratum: doi:10.1007/JHEP02(2010)011].
- [42] E. Re, “Single-top Wt-channel production matched with parton showers using the POWHEG method”, *Eur. Phys. J. C* **71** (2011) 1547, doi:10.1140/epjc/s10052-011-1547-z, arXiv:1009.2450.
- [43] J. Alwall et al., “The automated computation of tree-level and next-to-leading order differential cross sections, and their matching to parton shower simulations”, *JHEP* **07** (2014) 079, doi:10.1007/JHEP07(2014)079, arXiv:1405.0301.
- [44] T. Sjöstrand et al., “An Introduction to PYTHIA 8.2”, *Comput. Phys. Commun.* **191** (2015) 159, doi:10.1016/j.cpc.2015.01.024, arXiv:1410.3012.

- [45] W. Beenakker, R. Höpker, M. Spira, and P. M. Zerwas, “Squark and gluino production at hadron colliders”, *Nucl. Phys. B* **492** (1997) 51, doi:10.1016/S0550-3213(97)00084-9, arXiv:hep-ph/9610490.
- [46] A. Kulesza and L. Motyka, “Threshold resummation for squark-antisquark and gluino-pair production at the LHC”, *Phys. Rev. Lett.* **102** (2009) 111802, doi:10.1103/PhysRevLett.102.111802, arXiv:0807.2405.
- [47] A. Kulesza and L. Motyka, “Soft gluon resummation for the production of gluino-gluino and squark-antisquark pairs at the LHC”, *Phys. Rev. D* **80** (2009) 095004, doi:10.1103/PhysRevD.80.095004, arXiv:0905.4749.
- [48] W. Beenakker et al., “Soft-gluon resummation for squark and gluino hadroproduction”, *JHEP* **12** (2009) 041, doi:10.1088/1126-6708/2009/12/041, arXiv:0909.4418.
- [49] W. Beenakker et al., “Squark and gluino hadroproduction”, *Int. J. Mod. Phys. A* **26** (2011) 2637, doi:10.1142/S0217751X11053560, arXiv:1105.1110.
- [50] S. Agostinelli et al., “GEANT4 — a simulation toolkit”, *Nucl. Instr. and Meth. A* **506** (2003) 250, doi:10.1016/S0168-9002(03)01368-8.
- [51] CMS Collaboration, “The Fast Simulation of the CMS Detector at LHC”, in *Int'l Conf. on Computing in High Energy and Nuclear Physics (CHEP 2010)*. 2011. Journal of Physics: Conference Series, 331 (2011), 032049. doi:10.1088/1742-6596/331/3/032049.
- [52] CMS Collaboration, “Measurement of the Polarization of W Bosons with Large Transverse Momenta in W+Jets Events at the LHC”, *Phys. Rev. Lett.* **107** (2011) 021802, doi:10.1103/PhysRevLett.107.021802, arXiv:1104.3829.
- [53] ATLAS Collaboration, “Measurement of the Inelastic Proton-Proton Cross Section at $\sqrt{s} = 13$ TeV with the ATLAS Detector at the LHC”, (2016). arXiv:1606.02625. Submitted to *PRL*.
- [54] CMS Collaboration, “CMS Luminosity Measurement for the 2015 Data Taking Period”, CMS Physics Analysis Summary CMS-PAS-LUM-15-001, CERN, 2016.
- [55] CMS Collaboration, “Measurement of the production cross section of the W boson in association with two b jets in pp collisions at $\sqrt{s} = 8$ TeV”, (2016). arXiv:1608.07561. Submitted to EPJC.
- [56] CMS Collaboration, “Measurement of the differential cross section for top quark pair production in pp collisions at $\sqrt{s} = 8$ TeV”, *Eur. Phys. J. C* **75** (2015) 542, doi:10.1140/epjc/s10052-015-3709-x, arXiv:1505.04480.
- [57] Z. Bern et al., “Left-handed W bosons at the LHC”, *Phys. Rev. D* **84** (2011) 034008, doi:10.1103/PhysRevD.84.034008, arXiv:1103.5445.
- [58] CMS Collaboration, “Angular coefficients of Z bosons produced in pp collisions at $\sqrt{s} = 8$ TeV and decaying to $\mu^+\mu^-$ as a function of transverse momentum and rapidity”, *Phys. Lett. B* **750** (2015) 154, doi:10.1016/j.physletb.2015.08.061, arXiv:1504.03512.
- [59] ATLAS Collaboration, “Measurement of the polarisation of W bosons produced with large transverse momentum in pp collisions at $\sqrt{s} = 7$ TeV with the ATLAS experiment”, *Eur. Phys. J. C* **72** (2012) 2001, doi:10.1140/epjc/s10052-012-2001-6, arXiv:1203.2165.

- [60] CMS Collaboration, "Search for top-squark pair production in the single-lepton final state in pp collisions at $\sqrt{s} = 8 \text{ TeV}$ ", *Eur. Phys. J. C* **73** (2013) 2677, doi:10.1140/epjc/s10052-013-2677-2.
- [61] G. Cowan, K. Cranmer, E. Gross, and O. Vitells, "Asymptotic formulae for likelihood-based tests of new physics", *Eur. Phys. J. C* **71** (2011) 1554, doi:10.1140/epjc/s10052-011-1554-0, arXiv:1007.1727. [Erratum: doi:10.1140/epjc/s10052-013-2501-z].
- [62] T. Junk, "Confidence level computation for combining searches with small statistics", *Nucl. Instr. and Meth. A* **434** (1999) 435, doi:10.1016/S0168-9002(99)00498-2, arXiv:hep-ex/9902006.
- [63] A. L. Read, "Presentation of search results: the CL_s technique", *J. Phys. G* **28** (2002) 2693, doi:10.1088/0954-3899/28/10/313.

A The CMS Collaboration

Yerevan Physics Institute, Yerevan, Armenia

V. Khachatryan, A.M. Sirunyan, A. Tumasyan

Institut für Hochenergiephysik der OeAW, Wien, Austria

W. Adam, E. Asilar, T. Bergauer, J. Brandstetter, E. Brondolin, M. Dragicevic, J. Erö, M. Flechl, M. Friedl, R. Frühwirth¹, V.M. Ghete, C. Hartl, N. Hörmann, J. Hrubec, M. Jeitler¹, A. König, I. Krätschmer, D. Liko, T. Matsushita, I. Mikulec, D. Rabadý, N. Rad, B. Rahbaran, H. Rohringer, J. Schieck¹, J. Strauss, W. Treberer-Treberspurg, W. Waltenberger, C.-E. Wulz¹

National Centre for Particle and High Energy Physics, Minsk, Belarus

V. Mossolov, N. Shumeiko, J. Suarez Gonzalez

Universiteit Antwerpen, Antwerpen, Belgium

S. Alderweireldt, E.A. De Wolf, X. Janssen, J. Lauwers, M. Van De Klundert, H. Van Haevermaet, P. Van Mechelen, N. Van Remortel, A. Van Spilbeeck

Vrije Universiteit Brussel, Brussel, Belgium

S. Abu Zeid, F. Blekman, J. D'Hondt, N. Daci, I. De Bruyn, K. Deroover, N. Heracleous, S. Lowette, S. Moortgat, L. Moreels, A. Olbrechts, Q. Python, S. Tavernier, W. Van Doninck, P. Van Mulders, I. Van Parijs

Université Libre de Bruxelles, Bruxelles, Belgium

H. Brun, C. Caillol, B. Clerbaux, G. De Lentdecker, H. Delannoy, G. Fasanella, L. Favart, R. Goldouzian, A. Grebenyuk, G. Karapostoli, T. Lenzi, A. Léonard, J. Luetic, T. Maerschalk, A. Marinov, A. Randle-conde, T. Seva, C. Vander Velde, P. Vanlaer, R. Yonamine, F. Zenoni, F. Zhang²

Ghent University, Ghent, Belgium

A. Cimmino, T. Cornelis, D. Dobur, A. Fagot, G. Garcia, M. Gul, D. Poyraz, S. Salva, R. Schöfbeck, M. Tytgat, W. Van Driessche, E. Yazgan, N. Zaganidis

Université Catholique de Louvain, Louvain-la-Neuve, Belgium

H. Bakhshiansohi, C. Beluffi³, O. Bondu, S. Brochet, G. Bruno, A. Caudron, S. De Visscher, C. Delaere, M. Delcourt, B. Francois, A. Giammanco, A. Jafari, P. Jez, M. Komm, V. Lemaitre, A. Magitteri, A. Mertens, M. Musich, C. Nuttens, K. Piotrkowski, L. Quertenmont, M. Selvaggi, M. Vidal Marono, S. Wertz

Université de Mons, Mons, Belgium

N. Bely

Centro Brasileiro de Pesquisas Fisicas, Rio de Janeiro, Brazil

W.L. Aldá Júnior, F.L. Alves, G.A. Alves, L. Brito, C. Hensel, A. Moraes, M.E. Pol, P. Rebello Teles

Universidade do Estado do Rio de Janeiro, Rio de Janeiro, Brazil

E. Belchior Batista Das Chagas, W. Carvalho, J. Chinellato⁴, A. Custódio, E.M. Da Costa, G.G. Da Silveira⁵, D. De Jesus Damiao, C. De Oliveira Martins, S. Fonseca De Souza, L.M. Huertas Guativa, H. Malbouisson, D. Matos Figueiredo, C. Mora Herrera, L. Mundim, H. Nogima, W.L. Prado Da Silva, A. Santoro, A. Sznajder, E.J. Tonelli Manganote⁴, A. Vilela Pereira

Universidade Estadual Paulista ^a, Universidade Federal do ABC ^b, São Paulo, Brazil

S. Ahuja^a, C.A. Bernardes^b, S. Dogra^a, T.R. Fernandez Perez Tomei^a, E.M. Gregores^b,

P.G. Mercadante^b, C.S. Moon^a, S.F. Novaes^a, Sandra S. Padula^a, D. Romero Abad^b, J.C. Ruiz Vargas

Institute for Nuclear Research and Nuclear Energy, Sofia, Bulgaria

A. Aleksandrov, R. Hadjiiska, P. Iaydjiev, M. Rodozov, S. Stoykova, G. Sultanov, M. Vutova

University of Sofia, Sofia, Bulgaria

A. Dimitrov, I. Glushkov, L. Litov, B. Pavlov, P. Petkov

Beihang University, Beijing, China

W. Fang⁶

Institute of High Energy Physics, Beijing, China

M. Ahmad, J.G. Bian, G.M. Chen, H.S. Chen, M. Chen, Y. Chen⁷, T. Cheng, C.H. Jiang, D. Leggat, Z. Liu, F. Romeo, S.M. Shaheen, A. Spiezia, J. Tao, C. Wang, Z. Wang, H. Zhang, J. Zhao

State Key Laboratory of Nuclear Physics and Technology, Peking University, Beijing, China

Y. Ban, G. Chen, Q. Li, S. Liu, Y. Mao, S.J. Qian, D. Wang, Z. Xu

Universidad de Los Andes, Bogota, Colombia

C. Avila, A. Cabrera, L.F. Chaparro Sierra, C. Florez, J.P. Gomez, C.F. González Hernández, J.D. Ruiz Alvarez, J.C. Sanabria

University of Split, Faculty of Electrical Engineering, Mechanical Engineering and Naval Architecture, Split, Croatia

N. Godinovic, D. Lelas, I. Puljak, P.M. Ribeiro Cipriano, T. Sculac

University of Split, Faculty of Science, Split, Croatia

Z. Antunovic, M. Kovac

Institute Rudjer Boskovic, Zagreb, Croatia

V. Brigljevic, D. Ferencek, K. Kadija, S. Micanovic, L. Sudic, T. Susa

University of Cyprus, Nicosia, Cyprus

A. Attikis, G. Mavromanolakis, J. Mousa, C. Nicolaou, F. Ptochos, P.A. Razis, H. Rykaczewski

Charles University, Prague, Czech Republic

M. Finger⁸, M. Finger Jr.⁸

Universidad San Francisco de Quito, Quito, Ecuador

E. Carrera Jarrin

Academy of Scientific Research and Technology of the Arab Republic of Egypt, Egyptian Network of High Energy Physics, Cairo, Egypt

S. Elgammal⁹, A. Mohamed¹⁰

National Institute of Chemical Physics and Biophysics, Tallinn, Estonia

B. Calpas, M. Kadastik, M. Murumaa, L. Perrini, M. Raidal, A. Tiko, C. Veelken

Department of Physics, University of Helsinki, Helsinki, Finland

P. Eerola, J. Pekkanen, M. Voutilainen

Helsinki Institute of Physics, Helsinki, Finland

J. Härkönen, V. Karimäki, R. Kinnunen, T. Lampén, K. Lassila-Perini, S. Lehti, T. Lindén, P. Luukka, T. Peltola, J. Tuominiemi, E. Tuovinen, L. Wendland

Lappeenranta University of Technology, Lappeenranta, Finland

J. Talvitie, T. Tuuva

IRFU, CEA, Université Paris-Saclay, Gif-sur-Yvette, France

M. Besancon, F. Couderc, M. Dejardin, D. Denegri, B. Fabbro, J.L. Faure, C. Favaro, F. Ferri, S. Ganjour, S. Ghosh, A. Givernaud, P. Gras, G. Hamel de Monchenault, P. Jarry, I. Kucher, E. Locci, M. Machet, J. Malcles, J. Rander, A. Rosowsky, M. Titov, A. Zghiche

Laboratoire Leprince-Ringuet, Ecole Polytechnique, IN2P3-CNRS, Palaiseau, France

A. Abdulsalam, I. Antropov, S. Baffioni, F. Beaudette, P. Busson, L. Cadamuro, E. Chapon, C. Charlot, O. Davignon, R. Granier de Cassagnac, M. Jo, S. Lisniak, P. Miné, M. Nguyen, C. Ochando, G. Ortona, P. Paganini, P. Pigard, S. Regnard, R. Salerno, Y. Sirois, T. Strebler, Y. Yilmaz, A. Zabi

Institut Pluridisciplinaire Hubert Curien, Université de Strasbourg, Université de Haute Alsace Mulhouse, CNRS/IN2P3, Strasbourg, France

J.-L. Agram¹¹, J. Andrea, A. Aubin, D. Bloch, J.-M. Brom, M. Buttignol, E.C. Chabert, N. Chanon, C. Collard, E. Conte¹¹, X. Coubez, J.-C. Fontaine¹¹, D. Gelé, U. Goerlach, A.-C. Le Bihan, J.A. Merlin¹², K. Skovpen, P. Van Hove

Centre de Calcul de l'Institut National de Physique Nucleaire et de Physique des Particules, CNRS/IN2P3, Villeurbanne, France

S. Gadrat

Université de Lyon, Université Claude Bernard Lyon 1, CNRS-IN2P3, Institut de Physique Nucléaire de Lyon, Villeurbanne, France

S. Beauceron, C. Bernet, G. Boudoul, E. Bouvier, C.A. Carrillo Montoya, R. Chierici, D. Contardo, B. Courbon, P. Depasse, H. El Mamouni, J. Fan, J. Fay, S. Gascon, M. Gouzevitch, G. Grenier, B. Ille, F. Lagarde, I.B. Laktineh, M. Lethuillier, L. Mirabito, A.L. Pequegnot, S. Perries, A. Popov¹³, D. Sabes, V. Sordini, M. Vander Donckt, P. Verdier, S. Viret

Georgian Technical University, Tbilisi, Georgia

T. Toriashvili¹⁴

Tbilisi State University, Tbilisi, Georgia

Z. Tsamalaidze⁸

RWTH Aachen University, I. Physikalisches Institut, Aachen, Germany

C. Autermann, S. Beranek, L. Feld, A. Heister, M.K. Kiesel, K. Klein, M. Lipinski, A. Ostapchuk, M. Preuten, F. Raupach, S. Schael, C. Schomakers, J.F. Schulte, J. Schulz, T. Verlage, H. Weber, V. Zhukov¹³

RWTH Aachen University, III. Physikalisches Institut A, Aachen, Germany

M. Brodski, E. Dietz-Laursonn, D. Duchardt, M. Endres, M. Erdmann, S. Erdweg, T. Esch, R. Fischer, A. Güth, M. Hamer, T. Hebbeker, C. Heidemann, K. Hoepfner, S. Knutzen, M. Merschmeyer, A. Meyer, P. Millet, S. Mukherjee, M. Olschewski, K. Padeken, T. Pook, M. Radziej, H. Reithler, M. Rieger, F. Scheuch, L. Sonnenschein, D. Teyssier, S. Thüer

RWTH Aachen University, III. Physikalisches Institut B, Aachen, Germany

V. Cherepanov, G. Flügge, W. Haj Ahmad, F. Hoehle, B. Kargoll, T. Kress, A. Künsken, J. Lingemann, A. Nehr Korn, A. Nowack, I.M. Nugent, C. Pistone, O. Pooth, A. Stahl¹²

Deutsches Elektronen-Synchrotron, Hamburg, Germany

M. Aldaya Martin, C. Asawatangtrakuldee, K. Beernaert, O. Behnke, U. Behrens, A.A. Bin Anuar, K. Borras¹⁵, A. Campbell, P. Connor, C. Contreras-Campana, F. Costanza, C. Diez

Pardos, G. Dolinska, G. Eckerlin, D. Eckstein, E. Eren, E. Gallo¹⁶, J. Garay Garcia, A. Geiser, A. Gizhko, J.M. Grados Luyando, P. Gunnellini, A. Harb, J. Hauk, M. Hempel¹⁷, H. Jung, A. Kalogeropoulos, O. Karacheban¹⁷, M. Kasemann, J. Keaveney, J. Kieseler, C. Kleinwort, I. Korol, D. Krücker, W. Lange, A. Lelek, J. Leonard, K. Lipka, A. Lobanov, W. Lohmann¹⁷, R. Mankel, I.-A. Melzer-Pellmann, A.B. Meyer, G. Mittag, J. Mnich, A. Mussgiller, E. Ntomari, D. Pitzl, R. Placakyte, A. Raspereza, B. Roland, M.Ö. Sahin, P. Saxena, T. Schoerner-Sadenius, C. Seitz, S. Spannagel, N. Stefaniuk, K.D. Trippkewitz, G.P. Van Onsem, R. Walsh, C. Wissing

University of Hamburg, Hamburg, Germany

V. Blobel, M. Centis Vignali, A.R. Draeger, T. Dreyer, E. Garutti, D. Gonzalez, J. Haller, M. Hoffmann, A. Junkes, R. Klanner, R. Kogler, N. Kovalchuk, T. Lapsien, T. Lenz, I. Marchesini, D. Marconi, M. Meyer, M. Niedziela, D. Nowatschin, F. Pantaleo¹², T. Peiffer, A. Perieanu, J. Poehlsen, C. Sander, C. Scharf, P. Schleper, A. Schmidt, S. Schumann, J. Schwandt, H. Stadie, G. Steinbrück, F.M. Stober, M. Stöver, H. Tholen, D. Troendle, E. Usai, L. Vanelderen, A. Vanhoefer, B. Vormwald

Institut für Experimentelle Kernphysik, Karlsruhe, Germany

C. Barth, C. Baus, J. Berger, E. Butz, T. Chwalek, F. Colombo, W. De Boer, A. Dierlamm, S. Fink, R. Friese, M. Giffels, A. Gilbert, P. Goldenzweig, D. Haitz, F. Hartmann¹², S.M. Heindl, U. Husemann, I. Katkov¹³, P. Lobelle Pardo, B. Maier, H. Mildner, M.U. Mozer, T. Müller, Th. Müller, M. Plagge, G. Quast, K. Rabbertz, S. Röcker, F. Roscher, M. Schröder, I. Shvetsov, G. Sieber, H.J. Simonis, R. Ulrich, J. Wagner-Kuhr, S. Wayand, M. Weber, T. Weiler, S. Williamson, C. Wöhrmann, R. Wolf

Institute of Nuclear and Particle Physics (INPP), NCSR Demokritos, Aghia Paraskevi, Greece

G. Anagnostou, G. Daskalakis, T. Gerasis, V.A. Giakoumopoulou, A. Kyriakis, D. Loukas, I. Topsis-Giotis

National and Kapodistrian University of Athens, Athens, Greece

A. Agapitos, S. Kesisoglou, A. Panagiotou, N. Saoulidou, E. Tziaferi

University of Ioánnina, Ioánnina, Greece

I. Evangelou, G. Flouris, C. Foudas, P. Kokkas, N. Loukas, N. Manthos, I. Papadopoulos, E. Paradis

MTA-ELTE Lendület CMS Particle and Nuclear Physics Group, Eötvös Loránd University, Budapest, Hungary

N. Filipovic

Wigner Research Centre for Physics, Budapest, Hungary

G. Bencze, C. Hajdu, P. Hidas, D. Horvath¹⁸, F. Sikler, V. Veszpremi, G. Vesztergombi¹⁹, A.J. Zsigmond

Institute of Nuclear Research ATOMKI, Debrecen, Hungary

N. Beni, S. Czellar, J. Karancsi²⁰, A. Makovec, J. Molnar, Z. Szillasi

University of Debrecen, Debrecen, Hungary

M. Bartók¹⁹, P. Raics, Z.L. Trocsanyi, B. Ujvari

National Institute of Science Education and Research, Bhubaneswar, India

S. Bahinipati, S. Choudhury²¹, P. Mal, K. Mandal, A. Nayak²², D.K. Sahoo, N. Sahoo, S.K. Swain

Panjab University, Chandigarh, India

S. Bansal, S.B. Beri, V. Bhatnagar, R. Chawla, U. Bhawandeep, A.K. Kalsi, A. Kaur, M. Kaur, R. Kumar, A. Mehta, M. Mittal, J.B. Singh, G. Walia

University of Delhi, Delhi, India

Ashok Kumar, A. Bhardwaj, B.C. Choudhary, R.B. Garg, S. Keshri, S. Malhotra, M. Naimuddin, N. Nishu, K. Ranjan, R. Sharma, V. Sharma

Saha Institute of Nuclear Physics, Kolkata, India

R. Bhattacharya, S. Bhattacharya, K. Chatterjee, S. Dey, S. Dutt, S. Dutta, S. Ghosh, N. Majumdar, A. Modak, K. Mondal, S. Mukhopadhyay, S. Nandan, A. Purohit, A. Roy, D. Roy, S. Roy Chowdhury, S. Sarkar, M. Sharan, S. Thakur

Indian Institute of Technology Madras, Madras, India

P.K. Behera

Bhabha Atomic Research Centre, Mumbai, India

R. Chudasama, D. Dutta, V. Jha, V. Kumar, A.K. Mohanty¹², P.K. Netrakanti, L.M. Pant, P. Shukla, A. Topkar

Tata Institute of Fundamental Research-A, Mumbai, India

T. Aziz, S. Dugad, G. Kole, B. Mahakud, S. Mitra, G.B. Mohanty, B. Parida, N. Sur, B. Sutar

Tata Institute of Fundamental Research-B, Mumbai, India

S. Banerjee, S. Bhowmik²³, R.K. Dewanjee, S. Ganguly, M. Guchait, Sa. Jain, S. Kumar, M. Maity²³, G. Majumder, K. Mazumdar, T. Sarkar²³, N. Wickramage²⁴

Indian Institute of Science Education and Research (IISER), Pune, India

S. Chauhan, S. Dube, V. Hegde, A. Kapoor, K. Kothekar, A. Rane, S. Sharma

Institute for Research in Fundamental Sciences (IPM), Tehran, Iran

H. Behnamian, S. Chenarani²⁵, E. Eskandari Tadavani, S.M. Etesami²⁵, A. Fahim²⁶, M. Khakzad, M. Mohammadi Najafabadi, M. Naseri, S. Paktinat Mehdiabadi, F. Rezaei Hosseinabadi, B. Safarzadeh²⁷, M. Zeinali

University College Dublin, Dublin, Ireland

M. Felcini, M. Grunewald

INFN Sezione di Bari ^a, Università di Bari ^b, Politecnico di Bari ^c, Bari, Italy

M. Abbrescia^{a,b}, C. Calabria^{a,b}, C. Caputo^{a,b}, A. Colaleo^a, D. Creanza^{a,c}, L. Cristella^{a,b}, N. De Filippis^{a,c}, M. De Palma^{a,b}, L. Fiore^a, G. Iaselli^{a,c}, G. Maggi^{a,c}, M. Maggi^a, G. Miniello^{a,b}, S. My^{a,b}, S. Nuzzo^{a,b}, A. Pompili^{a,b}, G. Pugliese^{a,c}, R. Radogna^{a,b}, A. Ranieri^a, G. Selvaggi^{a,b}, L. Silvestris^{a,12}, R. Venditti^{a,b}, P. Verwilligen^a

INFN Sezione di Bologna ^a, Università di Bologna ^b, Bologna, Italy

G. Abbiendi^a, C. Battilana, D. Bonacorsi^{a,b}, S. Braibant-Giacomelli^{a,b}, L. Brigliadori^{a,b}, R. Campanini^{a,b}, P. Capiluppi^{a,b}, A. Castro^{a,b}, F.R. Cavallo^a, S.S. Chhibra^{a,b}, G. Codispoti^{a,b}, M. Cuffiani^{a,b}, G.M. Dallavalle^a, F. Fabbri^a, A. Fanfani^{a,b}, D. Fasanella^{a,b}, P. Giacomelli^a, C. Grandi^a, L. Guiducci^{a,b}, S. Marcellini^a, G. Masetti^a, A. Montanari^a, F.L. Navarria^{a,b}, A. Perrotta^a, A.M. Rossi^{a,b}, T. Rovelli^{a,b}, G.P. Siroli^{a,b}, N. Tosi^{a,b,12}

INFN Sezione di Catania ^a, Università di Catania ^b, Catania, Italy

S. Albergo^{a,b}, M. Chiorboli^{a,b}, S. Costa^{a,b}, A. Di Mattia^a, F. Giordano^{a,b}, R. Potenza^{a,b}, A. Tricomi^{a,b}, C. Tuve^{a,b}

INFN Sezione di Firenze ^a, Università di Firenze ^b, Firenze, Italy

G. Barbagli^a, V. Ciulli^{a,b}, C. Civinini^a, R. D'Alessandro^{a,b}, E. Focardi^{a,b}, V. Gori^{a,b}, P. Lenzi^{a,b}, M. Meschini^a, S. Paoletti^a, G. Sguazzoni^a, L. Viliani^{a,b,12}

INFN Laboratori Nazionali di Frascati, Frascati, Italy

L. Benussi, S. Bianco, F. Fabbri, D. Piccolo, F. Primavera¹²

INFN Sezione di Genova ^a, Università di Genova ^b, Genova, Italy

V. Calvelli^{a,b}, F. Ferro^a, M. Lo Vetere^{a,b}, M.R. Monge^{a,b}, E. Robutti^a, S. Tosi^{a,b}

INFN Sezione di Milano-Bicocca ^a, Università di Milano-Bicocca ^b, Milano, Italy

L. Brianza¹², M.E. Dinardo^{a,b}, S. Fiorendi^{a,b}, S. Gennai^a, A. Ghezzi^{a,b}, P. Govoni^{a,b}, M. Malberti, S. Malvezzi^a, R.A. Manzoni^{a,b,12}, B. Marzocchi^{a,b}, D. Menasce^a, L. Moroni^a, M. Paganoni^{a,b}, D. Pedrini^a, S. Pigazzini, S. Ragazzi^{a,b}, T. Tabarelli de Fatis^{a,b}

INFN Sezione di Napoli ^a, Università di Napoli 'Federico II' ^b, Napoli, Italy, Università della Basilicata ^c, Potenza, Italy, Università G. Marconi ^d, Roma, Italy

S. Buontempo^a, N. Cavallo^{a,c}, G. De Nardo, S. Di Guida^{a,d,12}, M. Esposito^{a,b}, F. Fabozzi^{a,c}, A.O.M. Iorio^{a,b}, G. Lanza^a, L. Lista^a, S. Meola^{a,d,12}, P. Paolucci^{a,12}, C. Sciacca^{a,b}, F. Thyssen

INFN Sezione di Padova ^a, Università di Padova ^b, Padova, Italy, Università di Trento ^c, Trento, Italy

P. Azzi^{a,12}, N. Bacchetta^a, M. Bellato^a, L. Benato^{a,b}, A. Boletti^{a,b}, R. Carlin^{a,b}, A. Carvalho Antunes De Oliveira^{a,b}, M. Dall'Osso^{a,b}, P. De Castro Manzano^a, T. Dorigo^a, U. Dosselli^a, F. Gasparini^{a,b}, A. Gozzelino^a, S. Lacaprara^a, M. Margoni^{a,b}, A.T. Meneguzzo^{a,b}, F. Montecassiano^a, J. Pazzini^{a,b,12}, N. Pozzobon^{a,b}, P. Ronchese^{a,b}, F. Simonetto^{a,b}, E. Torassa^a, S. Ventura^a, M. Zanetti, P. Zotto^{a,b}, A. Zucchetta^{a,b}, G. Zumerle^{a,b}

INFN Sezione di Pavia ^a, Università di Pavia ^b, Pavia, Italy

A. Braghieri^a, A. Magnani^{a,b}, P. Montagna^{a,b}, S.P. Ratti^{a,b}, V. Re^a, C. Riccardi^{a,b}, P. Salvini^a, I. Vai^{a,b}, P. Vitulo^{a,b}

INFN Sezione di Perugia ^a, Università di Perugia ^b, Perugia, Italy

L. Alunni Solestizi^{a,b}, G.M. Bilei^a, D. Ciangottini^{a,b}, L. Fanò^{a,b}, P. Lariccia^{a,b}, R. Leonardi^{a,b}, G. Mantovani^{a,b}, M. Menichelli^a, A. Saha^a, A. Santocchia^{a,b}

INFN Sezione di Pisa ^a, Università di Pisa ^b, Scuola Normale Superiore di Pisa ^c, Pisa, Italy

K. Androsov^{a,28}, P. Azzurri^{a,12}, G. Bagliesi^a, J. Bernardini^a, T. Boccali^a, R. Castaldi^a, M.A. Ciocci^{a,28}, R. Dell'Orso^a, S. Donato^{a,c}, G. Fedi, A. Giassi^a, M.T. Grippo^{a,28}, F. Ligabue^{a,c}, T. Lomtadze^a, L. Martini^{a,b}, A. Messineo^{a,b}, F. Palla^a, A. Rizzi^{a,b}, A. Savoy-Navarro^{a,29}, P. Spagnolo^a, R. Tenchini^a, G. Tonelli^{a,b}, A. Venturi^a, P.G. Verdini^a

INFN Sezione di Roma ^a, Università di Roma ^b, Roma, Italy

L. Barone^{a,b}, F. Cavallari^a, M. Cipriani^{a,b}, G. D'imperio^{a,b,12}, D. Del Re^{a,b,12}, M. Diemoz^a, S. Gelli^{a,b}, C. Jorda^a, E. Longo^{a,b}, F. Margaroli^{a,b}, P. Meridiani^a, G. Organtini^{a,b}, R. Paramatti^a, F. Preiato^{a,b}, S. Rahatlou^{a,b}, C. Rovelli^a, F. Santanastasio^{a,b}

INFN Sezione di Torino ^a, Università di Torino ^b, Torino, Italy, Università del Piemonte Orientale ^c, Novara, Italy

N. Amapane^{a,b}, R. Arcidiacono^{a,c,12}, S. Argiro^{a,b}, M. Arneodo^{a,c}, N. Bartosik^a, R. Bellan^{a,b}, C. Biino^a, N. Cartiglia^a, F. Cenna^{a,b}, M. Costa^{a,b}, R. Covarelli^{a,b}, A. Degano^{a,b}, N. Demaria^a, L. Finco^{a,b}, B. Kiani^{a,b}, C. Mariotti^a, S. Maselli^a, E. Migliore^{a,b}, V. Monaco^{a,b}, E. Monteil^{a,b}, M.M. Obertino^{a,b}, L. Pacher^{a,b}, N. Pastrone^a, M. Pelliccioni^a, G.L. Pinna Angioni^{a,b}, F. Ravera^{a,b},

A. Romero^{a,b}, M. Ruspa^{a,c}, R. Sacchi^{a,b}, K. Shchelina^{a,b}, V. Sola^a, A. Solano^{a,b}, A. Staiano^a, P. Traczyk^{a,b}

INFN Sezione di Trieste ^a, Università di Trieste ^b, Trieste, Italy

S. Belforte^a, M. Casarsa^a, F. Cossutti^a, G. Della Ricca^{a,b}, C. La Licata^{a,b}, A. Schizzi^{a,b}, A. Zanetti^a

Kyungpook National University, Daegu, Korea

D.H. Kim, G.N. Kim, M.S. Kim, S. Lee, S.W. Lee, Y.D. Oh, S. Sekmen, D.C. Son, Y.C. Yang

Chonbuk National University, Jeonju, Korea

A. Lee

Hanyang University, Seoul, Korea

J.A. Brochero Cifuentes, T.J. Kim

Korea University, Seoul, Korea

S. Cho, S. Choi, Y. Go, D. Gyun, S. Ha, B. Hong, Y. Jo, Y. Kim, B. Lee, K. Lee, K.S. Lee, S. Lee, J. Lim, S.K. Park, Y. Roh

Seoul National University, Seoul, Korea

J. Almond, J. Kim, H. Lee, S.B. Oh, B.C. Radburn-Smith, S.h. Seo, U.K. Yang, H.D. Yoo, G.B. Yu

University of Seoul, Seoul, Korea

M. Choi, H. Kim, H. Kim, J.H. Kim, J.S.H. Lee, I.C. Park, G. Ryu, M.S. Ryu

Sungkyunkwan University, Suwon, Korea

Y. Choi, J. Goh, C. Hwang, J. Lee, I. Yu

Vilnius University, Vilnius, Lithuania

V. Dudenas, A. Juodagalvis, J. Vaitkus

National Centre for Particle Physics, Universiti Malaya, Kuala Lumpur, Malaysia

I. Ahmed, Z.A. Ibrahim, J.R. Komaragiri, M.A.B. Md Ali³⁰, F. Mohamad Idris³¹, W.A.T. Wan Abdullah, M.N. Yusli, Z. Zolkapli

Centro de Investigacion y de Estudios Avanzados del IPN, Mexico City, Mexico

H. Castilla-Valdez, E. De La Cruz-Burelo, I. Heredia-De La Cruz³², A. Hernandez-Almada, R. Lopez-Fernandez, R. Magaña Villalba, J. Mejia Guisao, A. Sanchez-Hernandez

Universidad Iberoamericana, Mexico City, Mexico

S. Carrillo Moreno, C. Oropeza Barrera, F. Vazquez Valencia

Benemerita Universidad Autonoma de Puebla, Puebla, Mexico

S. Carpinteyro, I. Pedraza, H.A. Salazar Ibarguen, C. Uribe Estrada

Universidad Autónoma de San Luis Potosí, San Luis Potosí, Mexico

A. Morelos Pineda

University of Auckland, Auckland, New Zealand

D. Krofcheck

University of Canterbury, Christchurch, New Zealand

P.H. Butler

National Centre for Physics, Quaid-I-Azam University, Islamabad, Pakistan

A. Ahmad, M. Ahmad, Q. Hassan, H.R. Hoorani, W.A. Khan, M.A. Shah, M. Shoaib, M. Waqas

National Centre for Nuclear Research, Swierk, Poland

H. Bialkowska, M. Bluj, B. Boimska, T. Frueboes, M. Górski, M. Kazana, K. Nawrocki, K. Romanowska-Rybinska, M. Szleper, P. Zalewski

Institute of Experimental Physics, Faculty of Physics, University of Warsaw, Warsaw, Poland

K. Bunkowski, A. Byzuk³³, K. Doroba, A. Kalinowski, M. Konecki, J. Krolikowski, M. Misiura, M. Olszewski, M. Walczak

Laboratório de Instrumentação e Física Experimental de Partículas, Lisboa, Portugal

P. Bargassa, C. Beirão Da Cruz E Silva, A. Di Francesco, P. Faccioli, P.G. Ferreira Parracho, M. Gallinaro, J. Hollar, N. Leonardo, L. Lloret Iglesias, M.V. Nemallapudi, J. Rodrigues Antunes, J. Seixas, O. Toldaiev, D. Vadrucio, J. Varela, P. Vischia

Joint Institute for Nuclear Research, Dubna, Russia

S. Afanasiev, V. Alexakhin, M. Gavrilenko, I. Golutvin, I. Gorbunov, A. Kamenev, V. Karjavin, G. Kozlov, A. Lanev, A. Malakhov, V. Matveev^{34,35}, P. Moisev, V. Palichik, V. Perelygin, M. Savina, S. Shmatov, N. Skatchkov, V. Smirnov, A. Zarubin

Petersburg Nuclear Physics Institute, Gatchina (St. Petersburg), Russia

L. Chtchypounov, V. Golovtsov, Y. Ivanov, V. Kim³⁶, E. Kuznetsova³⁷, V. Murzin, V. Oreshkin, V. Sulimov, A. Vorobyev

Institute for Nuclear Research, Moscow, Russia

Yu. Andreev, A. Dermenev, S. Gninenko, N. Golubev, A. Karneyeu, M. Kirsanov, N. Krasnikov, A. Pashenkov, D. Tlisov, A. Toropin

Institute for Theoretical and Experimental Physics, Moscow, Russia

V. Epshteyn, V. Gavrilov, N. Lychkovskaya, V. Popov, I. Pozdnyakov, G. Safronov, A. Spiridonov, M. Toms, E. Vlasov, A. Zhokin

Moscow Institute of Physics and Technology

A. Bylinkin³⁵

National Research Nuclear University 'Moscow Engineering Physics Institute' (MEPhI), Moscow, Russia

M. Chadeeva³⁸, O. Markin, E. Tarkovskii

P.N. Lebedev Physical Institute, Moscow, Russia

V. Andreev, M. Azarkin³⁵, I. Dremin³⁵, M. Kirakosyan, A. Leonidov³⁵, S.V. Rusakov, A. Terkulov

Skobeltsyn Institute of Nuclear Physics, Lomonosov Moscow State University, Moscow, Russia

A. Baskakov, A. Belyaev, E. Boos, M. Dubinin³⁹, L. Dudko, A. Ershov, A. Gribushin, V. Klyukhin, O. Kodolova, I. Lokhtin, I. Miagkov, S. Obraztsov, S. Petrushanko, V. Savrin, A. Snigirev

Novosibirsk State University (NSU), Novosibirsk, Russia

V. Blinov⁴⁰, Y.Skovpen⁴⁰

State Research Center of Russian Federation, Institute for High Energy Physics, Protvino, Russia

I. Azhgirey, I. Bayshev, S. Bitioukov, D. Elumakhov, V. Kachanov, A. Kalinin, D. Konstantinov, V. Krychkin, V. Petrov, R. Ryutin, A. Sobol, S. Troshin, N. Tyurin, A. Uzunian, A. Volkov

University of Belgrade, Faculty of Physics and Vinca Institute of Nuclear Sciences, Belgrade, Serbia

P. Adzic⁴¹, P. Cirkovic, D. Devetak, M. Dordevic, J. Milosevic, V. Rekovic

Centro de Investigaciones Energéticas Medioambientales y Tecnológicas (CIEMAT), Madrid, Spain

J. Alcaraz Maestre, M. Barrio Luna, E. Calvo, M. Cerrada, M. Chamizo Llatas, N. Colino, B. De La Cruz, A. Delgado Peris, A. Escalante Del Valle, C. Fernandez Bedoya, J.P. Fernández Ramos, J. Flix, M.C. Fouz, P. Garcia-Abia, O. Gonzalez Lopez, S. Goy Lopez, J.M. Hernandez, M.I. Josa, E. Navarro De Martino, A. Pérez-Calero Yzquierdo, J. Puerta Pelayo, A. Quintario Olmeda, I. Redondo, L. Romero, M.S. Soares

Universidad Autónoma de Madrid, Madrid, Spain

J.F. de Trocóniz, M. Missiroli, D. Moran

Universidad de Oviedo, Oviedo, Spain

J. Cuevas, J. Fernandez Menendez, I. Gonzalez Caballero, J.R. González Fernández, E. Palencia Cortezon, S. Sanchez Cruz, I. Suárez Andrés, J.M. Vizán Garcia

Instituto de Física de Cantabria (IFCA), CSIC-Universidad de Cantabria, Santander, Spain

I.J. Cabrillo, A. Calderon, J.R. Castiñeiras De Saa, E. Curras, M. Fernandez, J. Garcia-Ferrero, G. Gomez, A. Lopez Virto, J. Marco, C. Martinez Rivero, F. Matorras, J. Piedra Gomez, T. Rodrigo, A. Ruiz-Jimeno, L. Scodellaro, N. Trevisani, I. Vila, R. Vilar Cortabitarte

CERN, European Organization for Nuclear Research, Geneva, Switzerland

D. Abbaneo, E. Auffray, G. Auzinger, M. Bachtis, P. Baillon, A.H. Ball, D. Barney, P. Bloch, A. Bocci, A. Bonato, C. Botta, T. Camporesi, R. Castello, M. Cepeda, G. Cerminara, M. D'Alfonso, D. d'Enterria, A. Dabrowski, V. Daponte, A. David, M. De Gruttola, F. De Guio, A. De Roeck, E. Di Marco⁴², M. Dobson, B. Dorney, T. du Pree, D. Duggan, M. Dünser, N. Dupont, A. Elliott-Peisert, S. Fartoukh, G. Franzoni, J. Fulcher, W. Funk, D. Gigi, K. Gill, M. Girone, F. Glege, D. Gulhan, S. Gundacker, M. Guthoff, J. Hammer, P. Harris, J. Hegeman, V. Innocente, P. Janot, H. Kirschenmann, V. Knünz, A. Kornmayer¹², M.J. Kortelainen, K. Kousouris, M. Krammer¹, P. Lecoq, C. Lourenço, M.T. Lucchini, L. Malgeri, M. Mannelli, A. Martelli, F. Meijers, S. Mersi, E. Meschi, F. Moortgat, S. Morovic, M. Mulders, H. Neugebauer, S. Orfanelli, L. Orsini, L. Pape, E. Perez, M. Peruzzi, A. Petrilli, G. Petrucciani, A. Pfeiffer, M. Pierini, A. Racz, T. Reis, G. Rolandi⁴³, M. Rovere, M. Ruan, H. Sakulin, J.B. Sauvan, C. Schäfer, C. Schwick, M. Seidel, A. Sharma, P. Silva, M. Simon, P. Sphicas⁴⁴, J. Steggemann, M. Stoye, Y. Takahashi, M. Tosi, D. Treille, A. Triossi, A. Tsirou, V. Veckalns⁴⁵, G.I. Veres¹⁹, N. Wardle, H.K. Wöhri, A. Zagodzinska³³, W.D. Zeuner

Paul Scherrer Institut, Villigen, Switzerland

W. Bertl, K. Deiters, W. Erdmann, R. Horisberger, Q. Ingram, H.C. Kaestli, D. Kotlinski, U. Langenegger, T. Rohe

Institute for Particle Physics, ETH Zurich, Zurich, Switzerland

F. Bachmair, L. Bäni, L. Bianchini, B. Casal, G. Dissertori, M. Dittmar, M. Donegà, P. Eller, C. Grab, C. Heidegger, D. Hits, J. Hoss, G. Kasieczka, P. Lecomte[†], W. Lustermann, B. Mangano, M. Marionneau, P. Martinez Ruiz del Arbol, M. Masciovecchio, M.T. Meinhard, D. Meister, F. Micheli, P. Musella, F. Nessi-Tedaldi, F. Pandolfi, J. Pata, F. Pauss, G. Perrin, L. Perrozzi, M. Quittnat, M. Rossini, M. Schönenberger, A. Starodumov⁴⁶, V.R. Tavolaro, K. Theofilatos, R. Wallny

Universität Zürich, Zurich, Switzerland

T.K. Aarrestad, C. Amsler⁴⁷, L. Caminada, M.F. Canelli, A. De Cosa, C. Galloni, A. Hinzmann, T. Hreus, B. Kilminster, C. Lange, J. Ngadiuba, D. Pinna, G. Rauco, P. Robmann, D. Salerno, Y. Yang

National Central University, Chung-Li, Taiwan

V. Candelise, T.H. Doan, Sh. Jain, R. Khurana, M. Konyushikhin, C.M. Kuo, W. Lin, Y.J. Lu, A. Pozdnyakov, S.S. Yu

National Taiwan University (NTU), Taipei, Taiwan

Arun Kumar, P. Chang, Y.H. Chang, Y.W. Chang, Y. Chao, K.F. Chen, P.H. Chen, C. Dietz, F. Fiori, W.-S. Hou, Y. Hsiung, Y.F. Liu, R.-S. Lu, M. Miñano Moya, E. Paganis, A. Psallidas, J.f. Tsai, Y.M. Tzeng

Chulalongkorn University, Faculty of Science, Department of Physics, Bangkok, Thailand

B. Asavapibhop, G. Singh, N. Srimanobhas, N. Suwonjandee

Cukurova University, Adana, Turkey

A. Adiguzel, S. Cerci⁴⁸, S. Damarseekin, Z.S. Demiroglu, C. Dozen, I. Dumanoglu, S. Girgis, G. Gokbulut, Y. Guler, E. Gurpinar, I. Hos, E.E. Kangal⁴⁹, O. Kara, A. Kayis Topaksu, U. Kiminsu, M. Oglakci, G. Onengut⁵⁰, K. Ozdemir⁵¹, B. Tali⁴⁸, H. Topakli⁵², S. Turkcapar, I.S. Zorbakir, C. Zorbilmez

Middle East Technical University, Physics Department, Ankara, Turkey

B. Bilin, S. Bilmis, B. Isildak⁵³, G. Karapinar⁵⁴, M. Yalvac, M. Zeyrek

Bogazici University, Istanbul, Turkey

E. Gülmez, M. Kaya⁵⁵, O. Kaya⁵⁶, E.A. Yetkin⁵⁷, T. Yetkin⁵⁸

Istanbul Technical University, Istanbul, Turkey

A. Cakir, K. Cankocak, S. Sen⁵⁹

Institute for Scintillation Materials of National Academy of Science of Ukraine, Kharkov, Ukraine

B. Grynyov

National Scientific Center, Kharkov Institute of Physics and Technology, Kharkov, Ukraine

L. Levchuk, P. Sorokin

University of Bristol, Bristol, United Kingdom

R. Aggleton, F. Ball, L. Beck, J.J. Brooke, D. Burns, E. Clement, D. Cussans, H. Flacher, J. Goldstein, M. Grimes, G.P. Heath, H.F. Heath, J. Jacob, L. Kreczko, C. Lucas, D.M. Newbold⁶⁰, S. Paramesvaran, A. Poll, T. Sakuma, S. Seif El Nasr-storey, D. Smith, V.J. Smith

Rutherford Appleton Laboratory, Didcot, United Kingdom

K.W. Bell, A. Belyaev⁶¹, C. Brew, R.M. Brown, L. Calligaris, D. Cieri, D.J.A. Cockerill, J.A. Coughlan, K. Harder, S. Harper, E. Olaiya, D. Petyt, C.H. Shepherd-Themistocleous, A. Thea, I.R. Tomalin, T. Williams

Imperial College, London, United Kingdom

M. Baber, R. Bainbridge, O. Buchmuller, A. Bundock, D. Burton, S. Casasso, M. Citron, D. Colling, L. Corpe, P. Dauncey, G. Davies, A. De Wit, M. Della Negra, R. Di Maria, P. Dunne, A. Elwood, D. Futyan, Y. Haddad, G. Hall, G. Iles, T. James, R. Lane, C. Laner, R. Lucas⁶⁰, L. Lyons, A.-M. Magnan, S. Malik, L. Mastrolorenzo, J. Nash, A. Nikitenko⁴⁶, J. Pela, B. Penning,

M. Pesaresi, D.M. Raymond, A. Richards, A. Rose, C. Seez, S. Summers, A. Tapper, K. Uchida, M. Vazquez Acosta⁶², T. Virdee¹², J. Wright, S.C. Zenz

Brunel University, Uxbridge, United Kingdom

J.E. Cole, P.R. Hobson, A. Khan, P. Kyberd, D. Leslie, I.D. Reid, P. Symonds, L. Teodorescu, M. Turner

Baylor University, Waco, USA

A. Borzou, K. Call, J. Dittmann, K. Hatakeyama, H. Liu, N. Pastika

The University of Alabama, Tuscaloosa, USA

O. Charaf, S.I. Cooper, C. Henderson, P. Rumerio

Boston University, Boston, USA

D. Arcaro, A. Avetisyan, T. Bose, D. Gastler, D. Rankin, C. Richardson, J. Rohlf, L. Sulak, D. Zou

Brown University, Providence, USA

G. Benelli, E. Berry, D. Cutts, A. Garabedian, J. Hakala, U. Heintz, J.M. Hogan, O. Jesus, E. Laird, G. Landsberg, Z. Mao, M. Narain, S. Piperov, S. Sagir, E. Spencer, R. Syarif

University of California, Davis, Davis, USA

R. Breedon, G. Breto, D. Burns, M. Calderon De La Barca Sanchez, S. Chauhan, M. Chertok, J. Conway, R. Conway, P.T. Cox, R. Erbacher, C. Flores, G. Funk, M. Gardner, W. Ko, R. Lander, C. Mclean, M. Mulhearn, D. Pellett, J. Pilot, F. Ricci-Tam, S. Shalhout, J. Smith, M. Squires, D. Stolp, M. Tripathi, S. Wilbur, R. Yohay

University of California, Los Angeles, USA

R. Cousins, P. Everaerts, A. Florent, J. Hauser, M. Ignatenko, D. Saltzberg, E. Takasugi, V. Valuev, M. Weber

University of California, Riverside, Riverside, USA

K. Burt, R. Clare, J. Ellison, J.W. Gary, G. Hanson, J. Heilman, P. Jandir, E. Kennedy, F. Lacroix, O.R. Long, M. Olmedo Negrete, M.I. Paneva, A. Shrinivas, H. Wei, S. Wimpenny, B. R. Yates

University of California, San Diego, La Jolla, USA

J.G. Branson, G.B. Cerati, S. Cittolin, M. Derdzinski, R. Gerosa, A. Holzner, D. Klein, V. Krutelyov, J. Letts, I. Macneill, D. Olivito, S. Padhi, M. Pieri, M. Sani, V. Sharma, S. Simon, M. Tadel, A. Vartak, S. Wasserbaech⁶³, C. Welke, J. Wood, F. Würthwein, A. Yagil, G. Zevi Della Porta

University of California, Santa Barbara - Department of Physics, Santa Barbara, USA

R. Bhandari, J. Bradmiller-Feld, C. Campagnari, A. Dishaw, V. Dutta, K. Flowers, M. Franco Sevilla, P. Geffert, C. George, F. Golf, L. Gouskos, J. Gran, R. Heller, J. Incandela, N. Mccoll, S.D. Mullin, A. Ovcharova, J. Richman, D. Stuart, I. Suarez, C. West, J. Yoo

California Institute of Technology, Pasadena, USA

D. Anderson, A. Apresyan, J. Bendavid, A. Bornheim, J. Bunn, Y. Chen, J. Duarte, J.M. Lawhorn, A. Mott, H.B. Newman, C. Pena, M. Spiropulu, J.R. Vlimant, S. Xie, R.Y. Zhu

Carnegie Mellon University, Pittsburgh, USA

M.B. Andrews, V. Azzolini, T. Ferguson, M. Paulini, J. Russ, M. Sun, H. Vogel, I. Vorobiev

University of Colorado Boulder, Boulder, USA

J.P. Cumalat, W.T. Ford, F. Jensen, A. Johnson, M. Krohn, T. Mulholland, K. Stenson, S.R. Wagner

Cornell University, Ithaca, USA

J. Alexander, J. Chaves, J. Chu, S. Dittmer, K. McDermott, N. Mirman, G. Nicolas Kaufman, J.R. Patterson, A. Rinkevicius, A. Ryd, L. Skinnari, L. Soffi, S.M. Tan, Z. Tao, J. Thom, J. Tucker, P. Wittich, M. Zientek

Fairfield University, Fairfield, USA

D. Winn

Fermi National Accelerator Laboratory, Batavia, USA

S. Abdullin, M. Albrow, G. Apollinari, S. Banerjee, L.A.T. Bauerdick, A. Beretvas, J. Berryhill, P.C. Bhat, G. Bolla, K. Burkett, J.N. Butler, H.W.K. Cheung, F. Chlebana, S. Cihangir[†], M. Cremonesi, V.D. Elvira, I. Fisk, J. Freeman, E. Gottschalk, L. Gray, D. Green, S. Grünendahl, O. Gutsche, D. Hare, R.M. Harris, S. Hasegawa, J. Hirschauer, Z. Hu, B. Jayatilaka, S. Jindariani, M. Johnson, U. Joshi, B. Klima, B. Kreis, S. Lammel, J. Linacre, D. Lincoln, R. Lipton, T. Liu, R. Lopes De Sá, J. Lykken, K. Maeshima, N. Magini, J.M. Marraffino, S. Maruyama, D. Mason, P. McBride, P. Merkel, S. Mrenna, S. Nahn, C. Newman-Holmes[†], V. O'Dell, K. Pedro, O. Prokofyev, G. Rakness, L. Ristori, E. Sexton-Kennedy, A. Soha, W.J. Spalding, L. Spiegel, S. Stoynev, N. Strobbe, L. Taylor, S. Tkaczyk, N.V. Tran, L. Uplegger, E.W. Vaandering, C. Vernieri, M. Verzocchi, R. Vidal, M. Wang, H.A. Weber, A. Whitbeck

University of Florida, Gainesville, USA

D. Acosta, P. Avery, P. Bortignon, D. Bourilkov, A. Brinkerhoff, A. Carnes, M. Carver, D. Curry, S. Das, R.D. Field, I.K. Furic, J. Konigsberg, A. Korytov, P. Ma, K. Matchev, H. Mei, P. Milenovic⁶⁴, G. Mitselmakher, D. Rank, L. Shchutska, D. Sperka, L. Thomas, J. Wang, S. Wang, J. Yelton

Florida International University, Miami, USA

S. Linn, P. Markowitz, G. Martinez, J.L. Rodriguez

Florida State University, Tallahassee, USA

A. Ackert, J.R. Adams, T. Adams, A. Askew, S. Bein, B. Diamond, S. Hagopian, V. Hagopian, K.F. Johnson, A. Khatiwada, H. Prosper, A. Santra, M. Weinberg

Florida Institute of Technology, Melbourne, USA

M.M. Baarmand, V. Bhopatkar, S. Colafranceschi⁶⁵, M. Hohlmann, D. Noonan, T. Roy, F. Yumiceva

University of Illinois at Chicago (UIC), Chicago, USA

M.R. Adams, L. Apanasevich, D. Berry, R.R. Betts, I. Bucinskaite, R. Cavanaugh, O. Evdokimov, L. Gauthier, C.E. Gerber, D.J. Hofman, P. Kurt, C. O'Brien, I.D. Sandoval Gonzalez, P. Turner, N. Varelas, H. Wang, Z. Wu, M. Zakaria, J. Zhang

The University of Iowa, Iowa City, USA

B. Bilki⁶⁶, W. Clarida, K. Dilsiz, S. Durgut, R.P. Gandrajula, M. Haytmyradov, V. Khristenko, J.-P. Merlo, H. Mermerkaya⁶⁷, A. Mestvirishvili, A. Moeller, J. Nachtman, H. Ogul, Y. Onel, F. Ozok⁶⁸, A. Penzo, C. Snyder, E. Tiras, J. Wetzel, K. Yi

Johns Hopkins University, Baltimore, USA

I. Anderson, B. Blumenfeld, A. Cocoros, N. Eminizer, D. Fehling, L. Feng, A.V. Gritsan, P. Maksimovic, M. Osherson, J. Roskes, U. Sarica, M. Swartz, M. Xiao, Y. Xin, C. You

The University of Kansas, Lawrence, USA

A. Al-bataineh, P. Baringer, A. Bean, S. Boren, J. Bowen, C. Bruner, J. Castle, L. Forthomme,

R.P. Kenny III, A. Kropivnitskaya, D. Majumder, W. Mcbrayer, M. Murray, S. Sanders, R. Stringer, J.D. Tapia Takaki, Q. Wang

Kansas State University, Manhattan, USA

A. Ivanov, K. Kaadze, S. Khalil, M. Makouski, Y. Maravin, A. Mohammadi, L.K. Saini, N. Skhirtladze, S. Toda

Lawrence Livermore National Laboratory, Livermore, USA

F. Rebassoo, D. Wright

University of Maryland, College Park, USA

C. Anelli, A. Baden, O. Baron, A. Belloni, B. Calvert, S.C. Eno, C. Ferraioli, J.A. Gomez, N.J. Hadley, S. Jabeen, R.G. Kellogg, T. Kolberg, J. Kunkle, Y. Lu, A.C. Mignerey, Y.H. Shin, A. Skuja, M.B. Tonjes, S.C. Tonwar

Massachusetts Institute of Technology, Cambridge, USA

D. Abercrombie, B. Allen, A. Apyan, R. Barbieri, A. Baty, R. Bi, K. Bierwagen, S. Brandt, W. Busza, I.A. Cali, Z. Demiragli, L. Di Matteo, G. Gomez Ceballos, M. Goncharov, D. Hsu, Y. Iiyama, G.M. Innocenti, M. Klute, D. Kovalskyi, K. Krajczar, Y.S. Lai, Y.-J. Lee, A. Levin, P.D. Luckey, A.C. Marini, C. McGinn, C. Mironov, S. Narayanan, X. Niu, C. Paus, C. Roland, G. Roland, J. Salfeld-Nebgen, G.S.F. Stephans, K. Sumorok, K. Tatar, M. Varma, D. Velicanu, J. Veverka, J. Wang, T.W. Wang, B. Wyslouch, M. Yang, V. Zhukova

University of Minnesota, Minneapolis, USA

A.C. Benvenuti, R.M. Chatterjee, A. Evans, A. Finkel, A. Gude, P. Hansen, S. Kalafut, S.C. Kao, Y. Kubota, Z. Lesko, J. Mans, S. Nourbakhsh, N. Ruckstuhl, R. Rusack, N. Tambe, J. Turkewitz

University of Mississippi, Oxford, USA

J.G. Acosta, S. Oliveros

University of Nebraska-Lincoln, Lincoln, USA

E. Avdeeva, R. Bartek, K. Bloom, D.R. Claes, A. Dominguez, C. Fangmeier, R. Gonzalez Suarez, R. Kamalieddin, I. Kravchenko, A. Malta Rodrigues, F. Meier, J. Monroy, J.E. Siado, G.R. Snow, B. Stieger

State University of New York at Buffalo, Buffalo, USA

M. Alyari, J. Dolen, J. George, A. Godshalk, C. Harrington, I. Iashvili, J. Kaisen, A. Kharchilava, A. Kumar, A. Parker, S. Rappoccio, B. Roozbahani

Northeastern University, Boston, USA

G. Alverson, E. Barberis, D. Baumgartel, A. Hortiangtham, B. Knapp, A. Massironi, D.M. Morse, D. Nash, T. Orimoto, R. Teixeira De Lima, D. Trocino, R.-J. Wang, D. Wood

Northwestern University, Evanston, USA

S. Bhattacharya, K.A. Hahn, A. Kubik, A. Kumar, J.F. Low, N. Mucia, N. Odell, B. Pollack, M.H. Schmitt, K. Sung, M. Trovato, M. Velasco

University of Notre Dame, Notre Dame, USA

N. Dev, M. Hildreth, K. Hurtado Anampa, C. Jessop, D.J. Karmgard, N. Kellams, K. Lannon, N. Marinelli, F. Meng, C. Mueller, Y. Musienko³⁴, M. Planer, A. Reinsvold, R. Ruchti, G. Smith, S. Taroni, M. Wayne, M. Wolf, A. Woodard

The Ohio State University, Columbus, USA

J. Alimena, L. Antonelli, J. Brinson, B. Bylsma, L.S. Durkin, S. Flowers, B. Francis, A. Hart, C. Hill, R. Hughes, W. Ji, B. Liu, W. Luo, D. Puigh, B.L. Winer, H.W. Wulsin

Princeton University, Princeton, USA

S. Cooperstein, O. Driga, P. Elmer, J. Hardenbrook, P. Hebda, D. Lange, J. Luo, D. Marlow, T. Medvedeva, K. Mei, M. Mooney, J. Olsen, C. Palmer, P. Piroué, D. Stickland, C. Tully, A. Zuranski

University of Puerto Rico, Mayaguez, USA

S. Malik

Purdue University, West Lafayette, USA

A. Barker, V.E. Barnes, S. Folgueras, L. Gutay, M.K. Jha, M. Jones, A.W. Jung, K. Jung, D.H. Miller, N. Neumeister, X. Shi, J. Sun, A. Svyatkovskiy, F. Wang, W. Xie, L. Xu

Purdue University Calumet, Hammond, USA

N. Parashar, J. Stupak

Rice University, Houston, USA

A. Adair, B. Akgun, Z. Chen, K.M. Ecklund, F.J.M. Geurts, M. Guilbaud, W. Li, B. Michlin, M. Northup, B.P. Padley, R. Redjimi, J. Roberts, J. Rorie, Z. Tu, J. Zabel

University of Rochester, Rochester, USA

B. Betchart, A. Bodek, P. de Barbaro, R. Demina, Y.t. Duh, T. Ferbel, M. Galanti, A. Garcia-Bellido, J. Han, O. Hindrichs, A. Khukhunaishvili, K.H. Lo, P. Tan, M. Verzetti

Rutgers, The State University of New Jersey, Piscataway, USA

J.P. Chou, E. Contreras-Campana, Y. Gershtein, T.A. Gómez Espinosa, E. Halkiadakis, M. Heindl, D. Hidas, E. Hughes, S. Kaplan, R. Kunnawalkam Elayavalli, S. Kyriacou, A. Lath, K. Nash, H. Saka, S. Salur, S. Schnetzer, D. Sheffield, S. Somalwar, R. Stone, S. Thomas, P. Thomassen, M. Walker

University of Tennessee, Knoxville, USA

M. Foerster, J. Heideman, G. Riley, K. Rose, S. Spanier, K. Thapa

Texas A&M University, College Station, USA

O. Bouhali⁶⁹, A. Celik, M. Dalchenko, M. De Mattia, A. Delgado, S. Dildick, R. Eusebi, J. Gilmore, T. Huang, E. Juska, T. Kamon⁷⁰, R. Mueller, Y. Pakhotin, R. Patel, A. Perloff, L. Perniè, D. Rathjens, A. Rose, A. Safonov, A. Tatarinov, K.A. Ulmer

Texas Tech University, Lubbock, USA

N. Akchurin, C. Cowden, J. Damgov, C. Dragoiu, P.R. Duderu, J. Faulkner, S. Kunori, K. Lamichhane, S.W. Lee, T. Libeiro, S. Undleeb, I. Volobouev, Z. Wang

Vanderbilt University, Nashville, USA

A.G. Delannoy, S. Greene, A. Gurrola, R. Janjam, W. Johns, C. Maguire, A. Melo, H. Ni, P. Sheldon, S. Tuo, J. Velkovska, Q. Xu

University of Virginia, Charlottesville, USA

M.W. Arenton, P. Barria, B. Cox, J. Goodell, R. Hirosky, A. Ledovskoy, H. Li, C. Neu, T. Sinthuprasith, X. Sun, Y. Wang, E. Wolfe, F. Xia

Wayne State University, Detroit, USA

C. Clarke, R. Harr, P.E. Karchin, P. Lamichhane, J. Sturdy

University of Wisconsin - Madison, Madison, WI, USA

D.A. Belknap, S. Dasu, L. Dodd, S. Duric, B. Gomber, M. Grothe, M. Herndon, A. Hervé, P. Klabbers, A. Lanaro, A. Levine, K. Long, R. Loveless, I. Ojalvo, T. Perry, G.A. Pierro, G. Polese, T. Ruggles, A. Savin, A. Sharma, N. Smith, W.H. Smith, D. Taylor, N. Woods

†: Deceased

- 1: Also at Vienna University of Technology, Vienna, Austria
- 2: Also at State Key Laboratory of Nuclear Physics and Technology, Peking University, Beijing, China
- 3: Also at Institut Pluridisciplinaire Hubert Curien, Université de Strasbourg, Université de Haute Alsace Mulhouse, CNRS/IN2P3, Strasbourg, France
- 4: Also at Universidade Estadual de Campinas, Campinas, Brazil
- 5: Also at Universidade Federal de Pelotas, Pelotas, Brazil
- 6: Also at Université Libre de Bruxelles, Bruxelles, Belgium
- 7: Also at Deutsches Elektronen-Synchrotron, Hamburg, Germany
- 8: Also at Joint Institute for Nuclear Research, Dubna, Russia
- 9: Now at British University in Egypt, Cairo, Egypt
- 10: Also at Zewail City of Science and Technology, Zewail, Egypt
- 11: Also at Université de Haute Alsace, Mulhouse, France
- 12: Also at CERN, European Organization for Nuclear Research, Geneva, Switzerland
- 13: Also at Skobeltsyn Institute of Nuclear Physics, Lomonosov Moscow State University, Moscow, Russia
- 14: Also at Tbilisi State University, Tbilisi, Georgia
- 15: Also at RWTH Aachen University, III. Physikalisches Institut A, Aachen, Germany
- 16: Also at University of Hamburg, Hamburg, Germany
- 17: Also at Brandenburg University of Technology, Cottbus, Germany
- 18: Also at Institute of Nuclear Research ATOMKI, Debrecen, Hungary
- 19: Also at MTA-ELTE Lendület CMS Particle and Nuclear Physics Group, Eötvös Loránd University, Budapest, Hungary
- 20: Also at University of Debrecen, Debrecen, Hungary
- 21: Also at Indian Institute of Science Education and Research, Bhopal, India
- 22: Also at Institute of Physics, Bhubaneswar, India
- 23: Also at University of Visva-Bharati, Santiniketan, India
- 24: Also at University of Ruhuna, Matara, Sri Lanka
- 25: Also at Isfahan University of Technology, Isfahan, Iran
- 26: Also at University of Tehran, Department of Engineering Science, Tehran, Iran
- 27: Also at Plasma Physics Research Center, Science and Research Branch, Islamic Azad University, Tehran, Iran
- 28: Also at Università degli Studi di Siena, Siena, Italy
- 29: Also at Purdue University, West Lafayette, USA
- 30: Also at International Islamic University of Malaysia, Kuala Lumpur, Malaysia
- 31: Also at Malaysian Nuclear Agency, MOSTI, Kajang, Malaysia
- 32: Also at Consejo Nacional de Ciencia y Tecnología, Mexico city, Mexico
- 33: Also at Warsaw University of Technology, Institute of Electronic Systems, Warsaw, Poland
- 34: Also at Institute for Nuclear Research, Moscow, Russia
- 35: Now at National Research Nuclear University 'Moscow Engineering Physics Institute' (MEPhI), Moscow, Russia
- 36: Also at St. Petersburg State Polytechnical University, St. Petersburg, Russia
- 37: Also at University of Florida, Gainesville, USA
- 38: Also at P.N. Lebedev Physical Institute, Moscow, Russia
- 39: Also at California Institute of Technology, Pasadena, USA
- 40: Also at Budker Institute of Nuclear Physics, Novosibirsk, Russia
- 41: Also at Faculty of Physics, University of Belgrade, Belgrade, Serbia
- 42: Also at INFN Sezione di Roma; Università di Roma, Roma, Italy

- 43: Also at Scuola Normale e Sezione dell'INFN, Pisa, Italy
- 44: Also at National and Kapodistrian University of Athens, Athens, Greece
- 45: Also at Riga Technical University, Riga, Latvia
- 46: Also at Institute for Theoretical and Experimental Physics, Moscow, Russia
- 47: Also at Albert Einstein Center for Fundamental Physics, Bern, Switzerland
- 48: Also at Adiyaman University, Adiyaman, Turkey
- 49: Also at Mersin University, Mersin, Turkey
- 50: Also at Cag University, Mersin, Turkey
- 51: Also at Piri Reis University, Istanbul, Turkey
- 52: Also at Gaziosmanpasa University, Tokat, Turkey
- 53: Also at Ozyegin University, Istanbul, Turkey
- 54: Also at Izmir Institute of Technology, Izmir, Turkey
- 55: Also at Marmara University, Istanbul, Turkey
- 56: Also at Kafkas University, Kars, Turkey
- 57: Also at Istanbul Bilgi University, Istanbul, Turkey
- 58: Also at Yildiz Technical University, Istanbul, Turkey
- 59: Also at Hacettepe University, Ankara, Turkey
- 60: Also at Rutherford Appleton Laboratory, Didcot, United Kingdom
- 61: Also at School of Physics and Astronomy, University of Southampton, Southampton, United Kingdom
- 62: Also at Instituto de Astrofísica de Canarias, La Laguna, Spain
- 63: Also at Utah Valley University, Orem, USA
- 64: Also at University of Belgrade, Faculty of Physics and Vinca Institute of Nuclear Sciences, Belgrade, Serbia
- 65: Also at Facoltà Ingegneria, Università di Roma, Roma, Italy
- 66: Also at Argonne National Laboratory, Argonne, USA
- 67: Also at Erzincan University, Erzincan, Turkey
- 68: Also at Mimar Sinan University, Istanbul, Istanbul, Turkey
- 69: Also at Texas A&M University at Qatar, Doha, Qatar
- 70: Also at Kyungpook National University, Daegu, Korea